"Automated program for the calculation of the quasiparticle energies with the GW approximation"

MAESTRÍA EN CIENCIAS (ÓPTICA)

Asesor(es): Dr. Bernardo Mendoza Santoyo

Estudiante: Cristian Camilo Montes Vargas

Agosto 2019
León, Guanajuato, México

The complete source code for the work featured in this thesis can be found on Github. Supplementary codes and data

AUTOMATED PROGRAM FOR THE CALCULATION OF THE QUASIPARTICLE ENERGIES WITH GW APPROXIMATION

by

Cristian C. Montes

Approved:

Dr. Bernardo Mendoza Santoyo
Thesis Advisor

Dr. Laura Elena Casandra Rosales Zárate
Reader

Dr. Joel Briones Hernández
Reader

Centro de Investigaciones en Óptica, A.C.
Loma del Bosque 115, León, Guanajuato, 37150, México
July 14, 2016

"If nature were not beautiful, it would not be worth knowing, and if nature were not worth knowing, life would not be worth living."

Henri Poincare

Abstract

This thesis presents a general description of a program that automatizes the calculation of the quasiparticle energies of crystalline systems, by using the GW approximation. In this context, G is a Green's function that describes the dynamic of an electron. W is the dynamical screen interaction between electrons in a homogeneous and polarizable medium. The automation of the program consists in computing important functions that are needed to calculate the quasiparticle energies. These functions are the charge density, wave functions, the polarizability and the self-energy. All these functions can be computed by the software Abinit. However, the computation of those functions are not automatized by Abinit. The program developed in this thesis allows one to compute the eigen-energies of the system by using Density Functional Theory, and the Local Density Approximation for exchange-correlation potential V_{xc}. The program calculates quasiparticle energies and the optical band of semiconductors. The program also calculates the quasiparticle energies, Fermi energy and spectral function of metals. We calculated the linear dielectric function with the quasiparticle energies, by using the Random Phase Approximation for polarizability. The results show that the linear dielectric function computed with the quasiparticle energies is in agreement with experiments for semiconductors. The results also show that the optical band gap computed with GW approximation is more precise respect to experiments, in comparison with the optical band gap predicted by the Density Functional theory.

I

————— I dedicate this work to my brothers and friends, who with their support and constant motivation have taught me to appreciate the small achievements of life —————

ACKNOWLEDGEMENTS

CONTENTS

LIST OF FIGURES

VII

LIST OF TABLES

1 INTRODUCTION

Outline

1.1 Generalities

Nowadays, computational calculations are one of the most important tools in scientific researches. Together with experiments and theory, computational modelings and numerical calculations represent a great part of the common day work in science, technology and education [1, 2]. Scientific research at computational level is very important due to two main reasons: first, experiments have limitations under certain circumstances (techniques, samples, etc); second, microscopic processes like phase transition mechanism and in general the understanding of physics are not experimentally measured. In the frame of material sciences *ab initio* programs for calculation of physical properties requires in many cases of computer equipment with high computing capacity. Due to that, programs based on molecular mechanics, as CHARMM and GROMACS, govern the calculation of physical properties of systems with many molecules or atoms but with low accuracy respect to real energy of the system [3, 4]. However, *ab initio* calculations are increasingly important because of the high computing capability that nowadays exist [5]. Furthermore, with methods of automation is possible

to increase the efficiency of the calculations.

The Density Functional Theory (DFT) is one of the most first principles methods, used to compute general physical properties of systems, based on the ground state. DFT in terms of the Kohn-Sham equation has predicted, with high accuracy, structural properties of crystalline solids and molecules, ground state energies and internal forces [6–8] . Other kind of phenomena that like lattice vibrations and electronic excited states have been computed by DFT, but with low accuracy respect to experiments [9]. These predictions come from the fact that Kohn-Sham equations do not allow us to obtain the exact solution of the many body Schrödinger equation. The Kohn-Sham wave functions are not the wave functions of each particle of the system; these do not have physical analog. In addition, Kohn-Sham equation does not consider neither new configurations of energy, due to the presence of more electrons or excitonic effects due to holes produced in excitation cases. Thus, electron affinity and ionization potential are understimated. This leads to the well-known band gap problem of solid state physics in the frame of DFT with errors close to 40% respect to experimental results. [10–15].

The difficulty mentioned above is largely overcome by the Many Body Perturbation Theory (MBPT). In this context electron-electron and electron-photon interactions, responsible of the main aspects of band structure in solids, are included in the formalism of Green's functions used in the MBPT. Here, the probability amplitude for the propagation of an added or removed electron in a many body system, is given by Green's function propagator [16–20]. Specifically, the electron-electron interaction is treated as an interaction between a charge particle and a whole rest of charge in the system. This assumption leads to the concept of quasiparticle, where one part of the energy of the quasiparticle is "screened" by the interaction with the rest of the total charge. Considerations about a general perturbation leads to the formulation of the five Hedin's coupled equations [21]. These five equations contain the complete information, about energy of the system including the perturbation. Hedin's equations focus on the calculation of a non-local, non-hermitian and time dependent self-energy operator Σ. This is calculated from Dyson's equation, that relates Σ with the the Green's function. The Vertex function Γ and polarization function -which determines the screened function W of the system- are present in Hedin's equations and they must be computed by performing a complete iterative calculation [18, 20, 21].

In order to verify the results of MBPT with physical properties of solids connection with DFT is necessary. Källén-Lehmann representation, of a one particle Green's function propagator in terms of wave functions, allows one to obtain a quasiparticle equation, that is similar to Kohn-Sham equation, except for an additional term that includes the Σ self-energy operator. In such a case, both the Kohn-Sham and Hedin's equation are solved iteratively with a Self Consistent Field method (SCF) [18, 20]. However, experimental results have demonstrated that a SCF solution of the Hedin's equation is not necessary for most systems [22]. Using Kohn-Sham wave functions, as a starting point in the Källen-Lehman representation, a quasiparticle equation is obtained. By using the Adler-Wiser expression for polarizability in the screeening function W and taking $\Gamma = 1$ for the vertex function, it is possible to simplify the procedure and obtain good results for the quasiparticle energies [23, 24]. This approximation for the solution of the Hedin's equations is known as GW

approximation, and presents an error below 10% with respect to the experimental results [10, 11].

However, from a computational point of view the GW approximation requires a computer equipment of high efficiency. For this reason, in order to calculate the band structure of certain materials the GW approximation is often used only at the Gamma point; and the conduction bands calculated with the Kohn-Sham equations are displaced rigidly with the new value of the energy obtained from GW approximation [12, 18]. This correction to the band structure is known commonly as scissor correction and it have given good results for different systems. But the problem with this approach is that bad results are obtained for other kind of semiconductors, and energy bands of metals do not match with experimental results [22, 25]. Furthermore, a more precise calculation of the polarizability -that is related to a sum over states of each k point in the Irreducible Brillouin Zone (IBZ)- is achieved with a number of well-converged k points and with quasiparticle energies instead of Kohn-Sham energies [8, 20].

Although programs like Yambo, QUANTUM EXPRESSO and Abinit [26–32] allow to calculate the GW approximation on metals and semiconductors, the procedure for doing the computation of the GW quasiparticle energies are frequently designed to compute only on one k point [5]. Since the work developed on this thesis contain a great part of calculation in the Abinit program, we particularly refer to this software. With Abinit is possible to compute the quasiparticle energies over a different k points, but good results are obtained only if a previous converged test have been carried out with another important parameters, as total energy of the system and number of energy bands. When GW approximation is used on a crystalline system, the quasiparticle energy and polarizability are calculated more directly in the reciprocal space. Taking into account the Block's theorem is possible to define a cut-off energy of a reciprocal vector sphere that is related to the Fourier expansion of the wave function. Hence, it is necessary to converge several parameters like cut-off energy for polarizability and self-energy operator, number of bands in the sum over states and cut-off energy of the first Kohn-Sham calculation of the wave function and energy of the ground state [8, 18, 20]. In this context Abinit is able to perform a convergence study over each parameter but with the exception (and recommendation) that each parameter should be converged separately: which requires more work and time. These several steps to achieve a well-converged result of the quasiparticle energy is time consuming and cumbersome. For this reason it is necessary to implement an automated algorithm that allows a complete calculation of the GW energies on enough k points within the IBZ.

The principal objective of this thesis is to design an program that automates all the steps involved in the computation of quasiparticle energies. This automation must includes convergence tests, generation of k-points, computation of the dynamical screening and self-energy. The algorithm must calculate the GW correction over the energy bands of enough k-points in order to evaluate the dielectric function of semiconductors and metals with quasiparticle energies.

1.2   Density functional theory

1.2.1   Kohn-Sham equation

DFT is the principal method used to calculate physical properties based on ground state energy. This method allows one to evaluate, with high accuracy, structural properties of crystalline systems, total energy and charge density of ground state. DFT is an alternative variational procedure to Schrödinger equation, where the functional of the electronic energy is minimized respect to charge density. The principal advantage of the theory is to avoid the calculation of the 3N variable function presented in the multi-particle Scrödinger equation for a system with N particles: still for systems with a few atoms or molecules, the solution of the exact Schrödinger equation is extremely expensive at the computational level. Therefore, instead of resolving the Scrödinger equation DFT focuses on the charge density that minimizes the energy. The main ideas of the theory are enunciated in two theorems that were proposed by Pierre Hohenberg and Walter Kohn in 1964 [33]. One of the theorems states that the energy is a functional of charge density given by the relation

$$E[\rho] = F[\rho] + \int \rho(\mathbf{r})v(\mathbf{r}), \tag{1.1}$$

where $\rho(\mathbf{r})$ is the charge density, $v(\mathbf{r})$ is the external potential and $F[\rho(\mathbf{r})]$ represents the universal functional, that contains the kinetic energy and the interactions between electrons in the system. Equation 1.1 also states that the external potential depends of charge density. The other theorem establishes that the charge density of the ground state minimizes the energy of the system, turning the situation in a variational problem. Shortly after the publication of the basis of DFT, Kohn and Lu Jeu Sham proposed a way of expressing the different functionals. Representing the kinetic energy functional, T, and the charge density, $\rho(\mathbf{r})$, in term of wave functions $\phi_n(\mathbf{r})$ as:

$$T = \sum_{n=1}^{N} \int d\mathbf{r}\phi_n^*(\mathbf{r})(-\frac{1}{2}\nabla^2)\phi_n(\mathbf{r}), \tag{1.2}$$

$$\rho(\mathbf{r}) = \sum_{n=1}^{N} |\phi(r)|^2, \tag{1.3}$$

and using the Born-Oppenheimer approximation, which does not take into account the kinetic energy of nuclei, and applying the variational principle, Kohn and Sham obtained the following equation:

$$\left(-\frac{\hbar}{2m}\nabla^2 + V_{eff}(\mathbf{r})\right)\phi_n(\mathbf{r}) = E_n\phi_n(\mathbf{r}). \tag{1.4}$$

The equation 1.4 is known as a Kohn-Sham equation and is solved in a self consistent field method (SCF) that minimizes the energy functional [34]. The first term in the first factor is the kinetic energy of the n-th electron and $V_{eff}(\mathbf{r})$ is the effective potential given by

$$V_{eff}(\mathbf{r}) = \int d\mathbf{r}'\frac{\rho(\mathbf{r'})}{|\mathbf{r}\text{-}\mathbf{r'}|} + \frac{\delta E_{xc}(\mathbf{r'})}{\delta\rho(\mathbf{r})} + V(\mathbf{r}). \tag{1.5}$$

Where the first term of equation 1.5is the energy due to the Coulomb interaction, the second one is the exchange-correlation potential V_{xc} in terms of E_{xc}, and the third term is the external potential. The accuracy of the ground state energy is highly dependent of the exchange-correlation energy functional. One of the challenge of DFT is to find an expression for E_{xc} and this determines the type of approximation used in the DFT frame. The most common approximation used for E_{xc} is known as local density approximation (LDA) and is given by

$$E_{xc}^{LDA} = \int d\mathbf{r} \rho(\mathbf{r}) \epsilon_{xc}(\mathbf{r}), \tag{1.6}$$

where ϵ_{xc} is the exchange-correlation energy of a uniform electron gas [35]. In this work the approximation taken for the exchange-correlation energy is the LDA approximation. The LDA approximation for the exchange-correlation potential is constructed, by considering the dynamic of the electron in the crystal, as a fermion gas. The LDA is local because the value of the energy only depends of the point where the energy is evaluated [6, 35]. For this reason the eigen-energies, wave functions and linear dielectric function calculated with Kohn-Sham equation, that is, Kohn-Sham eigen-energies, Kohn-Sham wave functions and linear dielectric function ϵ are sometimes referred as $E_{n\mathbf{k}}^{LDA}$, $\phi_{n\mathbf{k}}^{LDA}$ and ϵ^{LDA}.

The wave functions $\phi_n(\mathbf{r})$ in 1.4 are not the real solutions for the wave functions of each electron, these wave functions do not have real physical meaning. However, the eigen-energies obtained for $\phi_n(\mathbf{r})$ can be taken as a good approximation to the energy bands of crystalline and molecular systems. In solid state physics, the Kohn-Sham equation is re-written in terms of the wave functions $\phi_{n\mathbf{k}}(\mathbf{r})$. In this context, equation 1.4 is solved for each electron and for each k-point in the IBZ of the reciprocal space. Here the use of Block's theorem for periodic systems allows to express the wave functions as an expansion of plane waves multiplied by a periodic function, and a Fourier transform of this periodic function is used to take advantage of the symmetry properties of crystalline systems:

$$\phi_{n\mathbf{k}}(\mathbf{r}) = e^{i\mathbf{k}\mathbf{r}} u_{n\mathbf{k}}(\mathbf{r}), \tag{1.7}$$

$$u_{n\mathbf{k}}(\mathbf{r}) = \sum_{\mathbf{G}} u_{n\mathbf{k}}(\mathbf{G}) e^{i\mathbf{G}\mathbf{r}}, \tag{1.8}$$

where $u_{n\mathbf{k}}(\mathbf{G})$ are the Fourier coefficients given by

$$u_{n\mathbf{k}}(\mathbf{G}) = \frac{1}{\Omega} \int_{\Omega} u_{n\mathbf{k}}(\mathbf{r}) e^{-i\mathbf{G}\mathbf{r}} d\mathbf{r}. \tag{1.9}$$

$\mathbf{G}$ vectors are k-vectors in reciprocal space, Ω is the volume of the unitary cell in the the IBZ and $u_{n\mathbf{k}}(\mathbf{G})$ decreases exponentially with kinetic energy $(\mathbf{k} + \mathbf{G})^2/2$. This last factor is known as the energy cut of the system, and determines the number of plane waves required in the expansion of the wave functions.

From a computational point of view, the Kohn-Sham equation are represented in a matrix equation of the form

$$\hat{F}_{\mu\nu}^{KS}\hat{C} = \hat{S}\hat{C}\hat{E}, \tag{1.10}$$

where the $\hat{F}_{\mu\nu}^{KS}$ contains the information about energy functionals given in the equations 1.2 and 1.5, $\hat{C}$ represents the Fourier coefficients of the Fourier transform of the wave functions in the reciprocal space, $\hat{S}$ is the overlap matrix, and $\hat{E}$ contains the eigen-energies of the wave functions $\phi_{n\mathbf{k}}(\mathbf{r})$ for each k-point in the IBZ. Typically, the procedure to achieve convergences in energy with a SCF method starts with a proposal wave function $u_{n\mathbf{k}}(\mathbf{G})$, then a Fast Fourier Transform (FFT) is done to optimize the matrix transformation required to obtained the wave function in the real space. Next, the density is calculated in real space and a FFT takes the density to reciprocal space. After that, the functionals are evaluated, the total ground state energy is calculated and new wave functions are found. With these new wave functions the procedure starts again and the energy found is compared with that of the previous iteration. This procedure is repeated until a desired convergence is obtained.

1.2.2 Band Gap problem in DFT

It is well known that the accuracy of DFT to predict the Band Gap of semiconductors is around 40% to 50% below comparison with experimental results [10–12]. This is a consequence that Kohn-Sham equations does not take into account the changes in band energies, due to the presence of other charges, or due to the rearrangement of valence bands when a valence electron is excited to a conduction band. By definition, the energy band gap is the difference between the ionization potential and electron affinity, or mathematically

$$E_{gap} = [E_{N+1} - E_N] - [E_N - E_{N-1}], \tag{1.11}$$

where E_{N+1} is the total energy of the system when an additional charge is present, and E_{N-1} is the total energy of the system when a charge is absent. Equation 1.11 gives the exact band gap of the system while the band gap obtained from Kohn-Sham equation only takes into account band energies with the same number of electrons. Comparing the equation 1.11 with Kohn-Sham band gap results in:

$$E_{gap} = E_{gap}^{KS} + \Delta_{xc}, \tag{1.12}$$

where Δ_{xc} is an additional energy necessary to acquire the exact band gap.

1.3 Many body perturbation theory

1.3.1 Dyson's equation

Many Body Perturbation Theory was developed as a method to understand the nature of the propagation of particles in space, when they are involved in some kind of interaction with other particles. In systems with many particles is necessary to have into account, in addition to the energy related to interaction with other particles, the energy of the interaction of particle with itself. This

kind of dynamical problem was the basis of quantum electrodynamics and then, to quantum field theory (QFT). Although the theory was developed in the context of quantum electrodynamics by Schwinger, Tomonaga and Feynman [36–38], the methods developed by Dyson and Hedin for systems with many particles, were also used in the field of condensed matter, giving good results [21, 39]. A good method to resolve the many body perturbation problem developed by Feynman was proposed by Dyson and Schwinger. They suggested to resolve the equation of quantized fields with Green's functions [40, 41]. Specifically, the function that describes the propagation of one electron between the space-time points $(\mathbf{r'}, t')$ and $(\mathbf{r}, t)$, in the N-th state of energy is a Green's function given by

$$G(\mathbf{r}, t; \mathbf{r}', t') = -i \langle N|T[\Psi(\mathbf{r}, t)\Psi^\dagger(\mathbf{r}', t')]|N\rangle, \tag{1.13}$$

where T is the time-ordering operator and $\Psi(\mathbf{r}, t)$ and $\Psi^\dagger(\mathbf{r}, t)$ are field operators of the form

$$\Psi(\mathbf{r}, t) = \sum_k u(\mathbf{r}, t)a_k, \tag{1.14a}$$

$$\Psi^\dagger(\mathbf{r}, t) = \sum_k u(\mathbf{r}, t)a_k^\dagger, \tag{1.14b}$$

being a_k and $a_k^\dagger$ the creator and annihilator operator respectively. The Green's function 1.13 is also known as zero-order Green's function. The fields operator Ψ and $\Psi^\dagger$ are responsible of the creation and annihilation of one electron in a N-state energy in a space-time interval. In a system with an interaction hamiltonian $\mathbf{H}_{int}$ the Green's function 1.13 is modified to include an time evolution operator $S(\infty)$ given by [40]

$$S(\infty) = S(t, t_0) = T[\exp(-i \int_{-\infty}^{\infty} dt' \mathbf{H}_{int})], \tag{1.15}$$

and the Green's function becomes

$$G(\mathbf{r}, t; \mathbf{r'}, t') = \frac{\langle N|T[\Psi(\mathbf{r}, t)\Psi^\dagger(\mathbf{r'}, t')S(\infty)]|N\rangle}{\langle S(\infty)\rangle}. \tag{1.16}$$

Expanding in series the $S(\infty)$ operator given in the equation 1.15, and replacing in the equation 1.16 and considering $\mathbf{H}_{int}$ as Coulomb interaction, an infinite series of terms that include several products of field operators are obtained. Using Wick's theorem is possible to represent those field operator products in terms of pair of products of the form

$$\langle T[\hat{O}_1\hat{O}_2...\hat{O}_n]\rangle = \pm\sum_p \langle T[\hat{O}_1\hat{O}_2]\rangle \langle T[\hat{O}_4\hat{O}_2]\rangle ... \langle T[\hat{O}_{n-1}\hat{O}_n]\rangle, \tag{1.17}$$

which results in an infinite series of products of zero-order Green's functions. However, these infinite terms that comes from the denominator of the equation 1.16, are canceled out with another infinite series terms of the numerator, that also includes only products of zero-order Green's functions. This procedure in which an infinite amount of terms is canceled out with another one is known as renormalization. Usually, expression 1.16 is renormalized using the method of Feynman diagrams. There, the terms that contain only zero-order Green's functions are disconnected diagrams in the sense that the particle does not interact with another ones. Consequently, the full dynamic of the

propagation of the particle is described only by connected diagrams, which represents interactions with the rest of fields and particles. If we adopt the notation $1 = (r_1; t_1)$, the expansion of the Green's function of the equation 1.16, by using equations 1.15 and 1.16, leads to an iterative equation of the form:

$$G(1,2) = G_0(1,2) + \int d3d4 G_0(1,3)\Sigma(3,4)G(4,2), \tag{1.18}$$

or in a simpler form

$$G = G_0 + G_0\Sigma G, \tag{1.19}$$

which is known as the Dyson's equation. Equation 1.18 shows that the many body perturbation problem, for the special case of electrons interacting among them, leads to an iterative equation, where the Σ factor is the self-energy operator and this is determined by Green and Coulomb functions.

1.3.2 Hedin's equations

The Scrödinger equation written in terms of Green's functions is given by

$$(i\frac{\partial}{\partial t} - \hat{H})G(\mathbf{r},\mathbf{t};\mathbf{r}',\mathbf{t}') + i\int d\mathbf{r}'' V_c(\mathbf{r},\mathbf{r}'') \langle N|\hat{\Psi}^\dagger(\mathbf{r}'',t)\hat{\Psi}(\mathbf{r}'',t)\hat{\Psi}(\mathbf{r},t)\hat{\Psi}^\dagger(\mathbf{r},t)|N\rangle$$
$$= \delta(\mathbf{r}-\mathbf{r}')\delta(t-t'), \quad (1.20)$$

where V_c is the Coulomb interaction, G is the Green's function of equation 1.19, and Ψ and $\Psi^\dagger$ are the field operators of equations 1.14. Using Dyson's equation 1.19 in equation 1.20, and on performing the corresponding calculations a system of five couple equation is obtained. These equations are known as Hedin's equations and are solved in an iterative way [21]. The five coupled equations are

$$G(1,2) = G_0(1,2) + \int d3d4 G_0(1,3)\Sigma(3,4)G(4,2), \tag{1.21a}$$

$$\Gamma(1,2,3) = \delta(1,3)\delta(1,2) + \int d4d5d6d7 \frac{\delta\Sigma(1,2)}{\delta G(4,5)}G(4,6)G(7,5)\Gamma(6,7,3), \tag{1.21b}$$

$$\chi(1,2) = -i\int d3d4 G(1,3)G(4,1)\Gamma(3,4,2), \tag{1.21c}$$

$$W(1,2) = V_c(1,2) + \int d3d4 V_c(2,4)\chi(4,3)W(1,3), \tag{1.21d}$$

$$\Sigma(1,2) = i\int d3d4 G(1,3)W(1,4)\Gamma(4,2,3). \tag{1.21e}$$

Equation 1.21a is the Dyson's equation, Γ in 1.21b is the vertex function of the coupling between the electron and a photon, χ in 1.21c is the linear polarizability, W in 1.21d is the dynamic screened Coulomb interaction between the electron and the rest of charges of the system, and Σ in 1.21e is the self-energy needed to compute the Green's function. Hence, the complete description of the dynamic of one-electron motion between the points $(\mathbf{r}', t')$ and $(\mathbf{r}, t)$ is determined by the equation 1.20, with Green's function G given by the equation 1.21a, which must be resolved iteratively by means the Hedin's equations 1.21. Schematically, the Hedin's equations can be represented by means of the Hedin pentagon as shown in the figure 1.1.
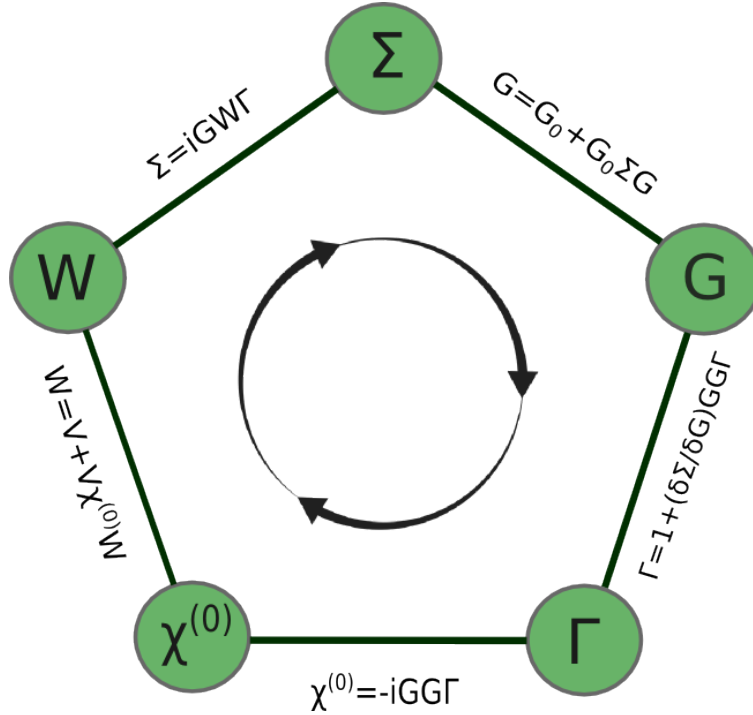
Figure 1.1: Hedin's pentagon

Usually, the first step for solving Hedin's equations, is to approximate the Green's function of the right hand side of equation 1.21a as:

$$G = G_0 + G_0 \Sigma G_0, \tag{1.22}$$

however, other consideration can be taken into account regarding with Γ or χ functions, and the equations are solved under a convergence criterion.

1.3.3 GW approximation

Hedin's equations has the particularity, from a numerical point of view, of being extremely difficult to compute due to the complex functions that are involved in the integral equations 1.21. For that

reason, approximations are done in order to resolve the Hedin's equations in a reasonable numerical way. The most common used approximation is the GW approximation. This approach considers the Γ function in the following form

$$\Gamma(1,2,3) = \delta(1,2)\delta(1,3), \tag{1.23}$$

which reduces the five coupled equations to four equations. In this context the remaining equations can be solved in an iterative procedure or can be solved in a one-shot computation starting from a given zero-order Green's function just as in the equation 1.22. Thus, the cyclic procedure of the Hedin pentagon of figure 1.1 can be visualized just as it appears in the figure 1.2.
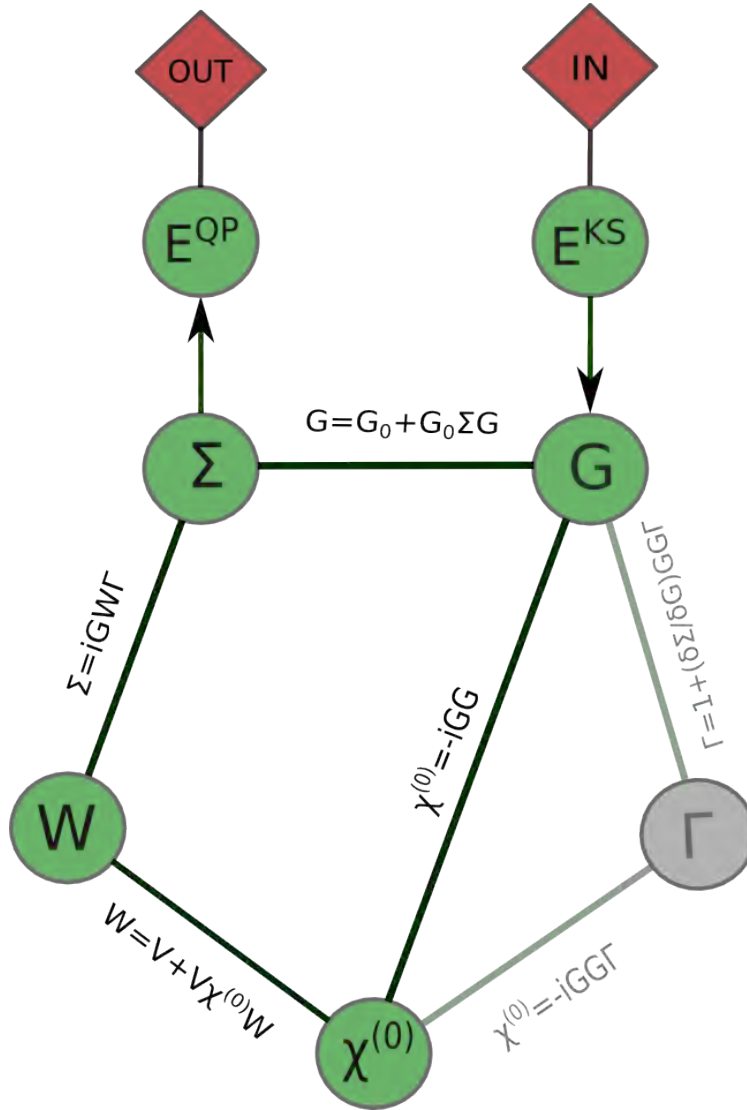
Figure 1.2: GW approximation in Hedin's pentagon

Hence, the equations for Σ and χ becomes

$$\Sigma(1,2) = iG(1,2)W(1,2), \tag{1.24a}$$

$$\chi(1,2) = -iG(1,2)G(2,1). \tag{1.24b}$$

The GW approximation takes its name from the form of the equation 1.24a, while the expression for χ in 1.24b is the RPA or independent particle approach for the polarizability of an electronic system in terms of Green's functions.

1.3.4 Connection with DFT

In order to do numerical calculations to compare with experiments a connection with DFT is necessary.Considering the Dyson's equation 1.18, the equation of motion of the one-particle Green's function in 1.20 can also be written as

$$[i\frac{\partial}{\partial t} - H_0]G(1,2) - \int d3\Sigma(1,3)G(3,2) = \delta(1,2), \tag{1.25}$$

where H_0 contains the kinetic energy, the Hartree potential and the external potential of the system. Equation 1.25 is known as the quasiparticle equation and comparing it with the Kohn-Sham equation 1.4 and with the equation 1.5 we have

$$\Sigma(\mathbf{r},t;\mathbf{r}',t';\epsilon) = V_{xc}(r,\rho(\mathbf{r}))\delta(\mathbf{r}-\mathbf{r}')\delta(t-t'). \tag{1.26}$$

Thus, the self-energy Σ is the exchange-correlation potential from the point of view of DFT and the dependence of Σ respect to ω, that is with quasiparticle energy, comes from the dependence of Σ respect to the Green's function as in equation 1.24a. To take advantage of the Kohn-Sham wave functions, the Källen-Lehmann representation is used in order to connect the Green's function with wave functions of DFT:

$$G(\mathbf{r},\mathbf{r}',\omega) = \sum_{n\mathbf{k}} \frac{\phi(\mathbf{r})\phi^*(\mathbf{r}')}{\omega - E_{n\mathbf{k}} + i\delta\mathrm{sgn}(E_{n\mathbf{k}} - \mu)}, \tag{1.27}$$

where μ is the chemical potential. The equation 1.27 allows to rewrite the quasiparticle equation 1.25 of the form

$$(-\frac{\nabla^2}{2} + V_{ext}(\mathbf{r}) + V_H(\mathbf{r}))\phi_{n\mathbf{k}}(\mathbf{r}) + \int d\mathbf{r}\Sigma(\mathbf{r},\mathbf{r}';E_{n\mathbf{k}}^{QP})\phi_{n\mathbf{k}}(\mathbf{r}') = E_{n\mathbf{k}}^{QP}\phi(\mathbf{r}). \tag{1.28}$$

Good results have been obtained for the case which wave functions $\phi_{n\mathbf{k}}$ and energies $\epsilon_{n\mathbf{k}}$ are approximated to Kohn-Sham wave functions and Kohn-Sham eigen-energies [42]. As a consequence of this last the quasiparticle energy (the real energy of the electron) is

$$E_{n\mathbf{k}}^{QP} = E_{n\mathbf{k}}^{KS} + \langle \phi_{n\mathbf{k}}^{KS}|\Sigma(\mathbf{r},\mathbf{r}',E_{n\mathbf{k}}^{QP}) - V_{xc}(\mathbf{r})|\phi_{n\mathbf{k}}^{KS}\rangle. \tag{1.29}$$

Then, to calculate the quasiparticle energy for each band energy is necessary to compute the Σ self-energy using the GW approximation with equations 1.24a and 1.24a. The expression 1.29 also

states that the band gap correction to DFT formalism, from the point of view of MBPT, is a correction that the potential V_{xc} does over the Σ operator.

1.4   RPA approximation for polarizability

The calculation of χ and W using equations 1.21d and 1.24b is performed by using the RPA. This is also known as the independent particle approximation (IPA) [7]. In this frame the polarizability of a crystalline system in reciprocal space is given by the equation

$$\chi_{\mathbf{G},\mathbf{G}'}(\mathbf{q},\omega) \;=\; 2\sum_{n,n',\mathbf{k}}(f_{n,\mathbf{k}}\;-\;f_{n',\mathbf{k}+\mathbf{q}})\frac{\langle\phi_{n',\mathbf{k}+\mathbf{q}}|e^{-i(\mathbf{q}+\mathbf{G})r}|\phi_{n',\mathbf{k}}\rangle\,\langle\phi_{n,\mathbf{k}}|e^{i(\mathbf{q}+\mathbf{G})r}|\phi_{n',\mathbf{k}+\mathbf{q}}\rangle}{E^{KS}_{n,\mathbf{k}}-E^{KS}_{n',\mathbf{k}+\mathbf{q}}-\omega-i\delta}, \quad (1.30)$$

which is the Adler-Wiser expression for polarizability [43]; and the linear dielectric function is

$$\epsilon^{RPA}_{\mathbf{G},\mathbf{G}'}(\mathbf{q},\omega) = \delta_{\mathbf{G},\mathbf{G}'} - V_{\mathbf{G}}(\mathbf{q})\chi_{\mathbf{G},\mathbf{G}'}(\mathbf{q},\omega). \tag{1.31}$$

where G and G' are vector in reciprocal space from the plane wave expansion and $\mathbf{q}$ are the k-point vectors in reciprocal space. The energies and the wave functions of the equation 1.30 are the eigen-energies and the eigen-states of the Kohn-Sham equation. These wave functions and energies are taken as a first approximation to compute the linear dielectric function using equations 1.30 and 1.31. Instead of taking the Kohn-Sham eigen-energies in the Adler-Wiser expression, one of the objectives of this thesis is to calculate the linear dielectric function of semiconductors and metals with the eigen-energies calculated with the GW approximation, that is, calculating the quasiparticle energies from equation 1.29. Once we get the energies $E^{QP}_{n\mathbf{k}}$ the dielectric function is computed with equations 1.30 and 1.31, then, it is not necessary to compute the quasiparticle eigen-states because $\phi_{n\mathbf{k}}(\mathbf{r})^{KS} \approx \phi_{n\mathbf{k}}(\mathbf{r})^{QP}$ as shown in [42, 44].

1.5   The GW approximation inside *Abinit* code

Abinit is a high efficiency code focused in physical properties from first principles. It has implemented several methods to improve time efficiency and precision of the calculations [28, 29]. The Abinit software allows one the calculation the quasiparticle energies of crystalline systems within the GW approximation. In this context the procedure to obtain the quasiparticles energies is given by four main steps. In the first two steps the density function and Kohn-Sham wave functions are calculated. In the third one, the inverse dielectric function and the dynamic screening function are computed. Finally the self-energy Σ is calculated and the quasiparticle energies are computed for each electron and each k-point in the IBZ using equation 1.29. Schematically the general procedure to get the quasiparticle energies is shown in the figure 1.3.

As it was just mentioned in the generalities section, some of the difficulties for calculating the quasiparticle energies are the convergence tests that are necessary to do to get high accuracy results. This convergence test must be done over different parameters and for each one of the four main steps
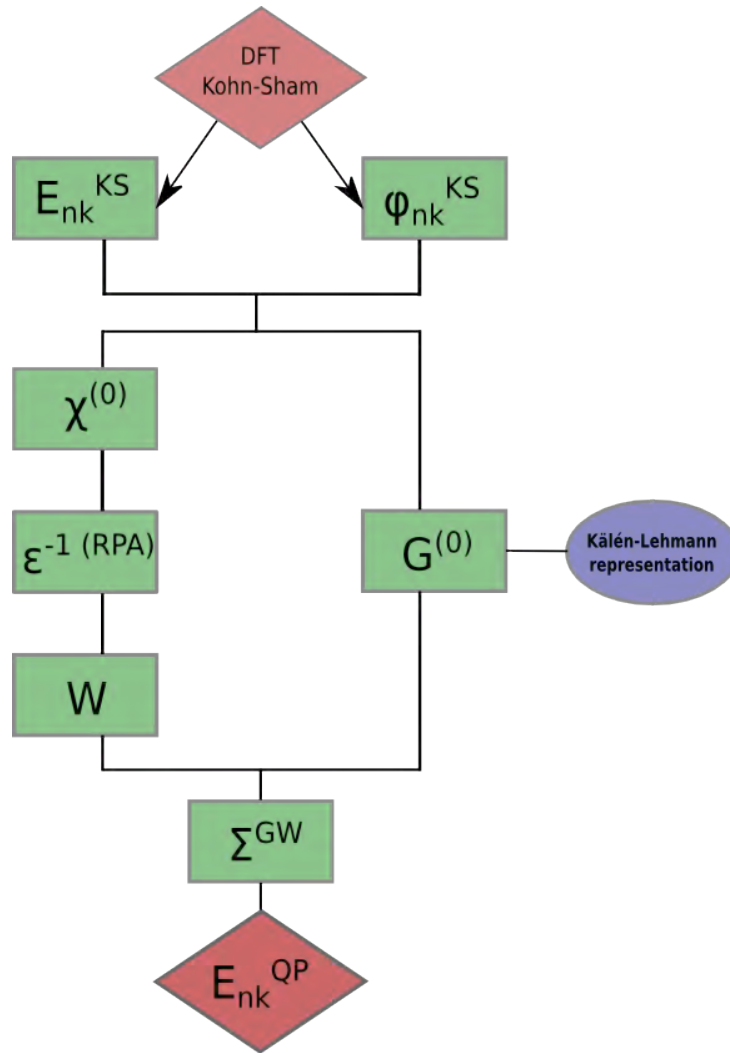
Figure 1.3: General steps in a calculation of the quasiparticle energies

mentioned above. Since a FFT is performed to calculate the Fourier coefficients, a convergence test for the number of plane waves is done in order to get the wave functions, the polarizability and the self-energy. In addition, the expressions implemented by Abinit for Σ and χ requires again a convergence test respect with number of band energies.

The first step consists in the calculation of the density with a SCF procedure under a specific convergence criterion. The wave functions computed in the second step are obtained by means of the charge density obtained in the first step, with a non self consistent field using the equation 1.10. The third step generates the polarizability trough equation 1.30 and the dynamical screening is computed with the following equation:

$$W_{\mathbf{G},\mathbf{G}'}(\mathbf{q},\omega) = \epsilon_{\mathbf{G},\mathbf{G}'}^{-1(RPA)}(\mathbf{q},\omega)V_{\mathbf{G}'}(\mathbf{q}), \tag{1.32}$$

where $V_{\mathbf{G}'}(\mathbf{q})$ is the Coulomb potential in reciprocal space given by

$$V_{\mathbf{G}'}(\mathbf{q}) = \sum_{\mathbf{G}'} \int \int d\mathbf{r} d\mathbf{r}' \rho(\mathbf{r})\rho(\mathbf{r}') \frac{e^{i(\mathbf{q}+\mathbf{G}')(\mathbf{r}-\mathbf{r}')}}{|\mathbf{q}+\mathbf{G}'|^2}. \tag{1.33}$$

The fourth step consists in calculating the self-energy Σ. Equation 1.29 relates the self-energy with exchange-correlation potential. A good approximation for the self-energy is to consider the relation $\Sigma_{xc} = \Sigma_x + \Sigma_c$ with

$$\langle\phi_{n,\mathbf{k}}|\Sigma_x|\phi_{n,\mathbf{k}}\rangle = -\frac{4\pi}{\Omega} \sum_v^{occ} \sum_q^{IBZ} \sum_G \frac{|M_{\mathbf{G}}^{n,n'}(\mathbf{k},\mathbf{q})|^2}{|\mathbf{q}+\mathbf{G}|^2} \tag{1.34a}$$

$$\langle\phi_{n,\mathbf{k}}|\Sigma_c|\phi_{n,\mathbf{k}}\rangle = \frac{i}{2\pi\Omega} \sum_{\mathbf{q}}^{IBZ} \sum_{\mathbf{G},\mathbf{G}'} \sum_{m=1}^{\infty} [M_{\mathbf{G}'}^{m,n}(\mathbf{k},\mathbf{q})]^* M_{\mathbf{G}'}^{m,n'}(\mathbf{k},\mathbf{q}) V_{\mathbf{G}\mathbf{G}'}(\mathbf{q}) J_{\mathbf{G}\mathbf{G}'}^{n,\mathbf{k}\text{-}\mathbf{q}}(\mathbf{q},\omega) \tag{1.34b}$$

where the sum in equation 1.34b is over occupied bands *occ*. $M_{\mathbf{G}'}^{m,n}(\mathbf{k},\mathbf{q})$ contains the momentum matrix element of the system given by

$$M_{\mathbf{G}'}^{m,n}(\mathbf{k},\mathbf{q}) = \langle\phi_{n',\mathbf{k}+\mathbf{q}}|e^{-i(\mathbf{q}+\mathbf{G})r}|\phi_{n',\mathbf{k}}\rangle. \tag{1.35}$$

This factor corresponds to the braket over plane waves that appears in the right hand side of equation 1.30 and is given by

$$M_{\mathbf{G}}^{m,n}(\mathbf{k},\mathbf{q}) = \langle\phi_{m,\mathbf{k}+\mathbf{q}}|e^{-i(\mathbf{q}+\mathbf{G})r}|\phi_{n,\mathbf{k}}\rangle \tag{1.36}$$

The expressions 1.34a and 1.34b show different summations. In 1.34a is necessary to converge the number of plane waves (G vectors) for each q-point vector and occupied bands. In 1.34b is necessary to converge the number of plane waves over an infinite number of bands for each q-point vector.

1.6   Outline

This thesis is divided into 4 chapters including this introduction. Chapter two explains the steps for the computation of quasiparticle energies and dielectric function. Furthermore, chapter two specifies the convergence tests, the generation of k-points, the edition of the files used and the utility of the automated program. In the third chapter different results are shown: dielectric function of some semiconductors and metals and spectral function of metallic systems. Chapter four contains the conclusions of the thesis, open questions and future work. An appendix is also presented with examples of a convergence test.

2 COMPUTATIONAL METHODOLOGY

Outline

2.1 The automated program

Abinit is a program that allows to compute the different functions and energies that are required in this work. Important functions and quantities, as the total energy, structural properties, wave functions, the ionization potential, band width of metals, the thermal and the electrical conductivity, the critic temperature of superconductors, and chemical energy bonds of molecules can also be computed Abinit [27,28,30]. But this procedure demands the calculation, step by step, of all parameters needed. All important functions like charge density, wave functions, screening and self energy, and important numerical values like total energy and quasiparticle energies are calculated with a good accuracy if a convergence test is done previously for different parameters. These convergence studies are done separately for each function and require time and work. Furthermore, the computation of the quasiparticle energies for a large number of k-points that are needed for a precise calculation of the dielectric function requires the previous generation of the k-points and a previous edition of the input files involved in the Abinit runs. All this procedure is required for a specific system and if it is necessary to compute another system the total procedure mentioned here must be done again.

As it was mentioned in the introduction, the main objective of this thesis is to develop a program that automatizes a complete calculation of the quasiparticle energies in order to compute

the dielectric function of metals and semiconductors. The program designed in this work includes convergence tests of parameters that are important in the computation of charge density, wave functions, screening and self-energy. The program also includes the generation of desired k-points for the computation of the screening and self-energy. And finally, the program generates an output file, with all quasiparticle energies for a specified number of bands and k-points. This file is used for the computation of the dielectric function with the TINIBA program [45].

The program has been designed focusing in the major efficiency, and the least possible work for the user, that is, the program is friendly user. The program automatizes the different procedures that are needed to get good results and is clear and simple for the user. The script is ran with the executable `GW.sh`. Before the script is ran, the user must know which are the basic parameters (primitive vectors, the atomic number, lattice parameter and the number of atom per cell) of the system that will be evaluated. When this script is ran, the screen shows a guide for starting a calculation and a list of crystalline systems available in the program, see figure 2.1. The guide indicates to the user that only has to introduce the tolerance criterion for the convergence studies, the number of cores for automatized parallelization, the grid for generation of k-points, the first conduction band, the nomenclature system, the Bravais lattice and another grid for optional interpolation. After the execution of the script the user must specify the principal parameters of the system. The general procedure can be summarized in the following steps

- Run the `GW.sh` script to start the automated program.

- Select the tolerance criterion `tol` for the convergence studies.

- Select the number of `cores` for the parallelization of the calculation.

- Select the dimension of the `grid` for generating the k-points mesh. The grid will have the same dimensions in all direction of the reciprocal space. Only one number is required.

- Select the number of bands `n_bands`.

- Specify the system `sys` with nomenclature symbols.

- Specify the kind of Bravais lattice (FCC, BCC, HL).

- Select an optional `grid2` to interpolate energies acquired with the k-points mesh of the parameter `grid`.

- Specify the principal parameters of the system (lattice constant, basis vectors, position of the atoms and nuclear charge)

When the user correctly specifies the arguments of the `GW.sh` script, the program starts to compute the complete procedure. The time of the calculation depends strongly of the size of the grid. When the script finishes a list of files that contains k-points list, quasiparticle energies and plots with energy bands are generated in a directory with the name `Sys-grid-n_kpt`; where `n_kpt` is the number of k-points generated by Abinit in the IBZ after the application of all symmetry

Figure 2.1: The guide for using `GW.sh`

matrices. Below is specified the functioning and the different steps of the program: convergence tests, computation of screening and self-energy, and finally the quasiparticle energies. All the algorithm of the program includes principally scripts in *bash*, *python* and *gnuplot* language.

2.2 Functioning of the *Abinit* code

Abinit requires a main file with extension .files, which specifies the names of other files that contains the input file with extension .in of a specific run, the name of the output file with extension .out where the results are shown, the names of the extensions of other files with important information of the results, and the names of the pseudopotentials that are used for a specific system. To run Abinit with the defined file .files is necessary that the input file contains the correct information about the system that will be evaluated. A basic input file contains information about the atoms,

lattice parameters, basis vectors in reciprocal space, number of k-points and energy cut of the system. In this work different input files are defined in order to compute different functions such as charge density, wave functions, screening and self-energy. For the calculation of the ground charge density is necessary to put, apart of the basic parameters, the energy cut (ecut). For wave functions is necessary to specify the number of bands (nband) that will be calculated. For screening and self-energy, number of bands and energy cut must be defined.

For the calculation of the different functions (charge density, wave functions, screening and self-energy) the Abinit output files contain relevant information that is used by the automation program made in this work. For ground charge density, the output files gives the total energy of the system and the charge density; for wave functions, the output files contains the coefficients of the wave functions of the expansion 1.8. For screening one of the output files is the dynamic screening matrix and for Self-energy, the output files contains the quasiparticle energies of specific bands defined in the input file.

Since several Abinit runs are done in the automated program, different input files are defined in order to compute convergence of parameters, charge density, wave functions, screening and self-energy. However, all these input files require the same basic information about the system that is evaluated. For this reason, a file with that basic information is edited by the user at the beginning of the run of the automation program. This file contains the lattice parameters, the type and number of atoms, position of the atoms, and basis vectors. As an example the basic parameters of the Si are shown in the following text:

```
#lattice parameters and basic vectors
acell  3*10.217
rprim  0.0  0.5  0.5
       0.5  0.0  0.5
       0.5  0.5  0.0

#Definition of the atom type
ntypat 1
znucl 14

#Definition of the atoms
natom 2
typat 1 1

#positions of the atoms
xred
   0.0  0.0  0.0
   1/4  1/4  1/4
```

This text file is added to all input files that the program uses in the automated program. In the context of the present work, if the system that will be evaluated has been calculated before, the

last text with the basic information will be saved in the data base of the program. Thus, the user does not have to edit anything. Other file with the pseudopotentials is also added to the file .files of each run. The code asks for the name of the pseudopotentials before of an calculation and those are saved in the data base of the program. However, if the pseudontentials have already been saved before, the user does not have to write them down. All that operations that add text files as those one containing basic parameters and pseudopotentials are executed in the code of the automated program with bash commands like `sed` or `awk`. These commands allows to put text files in a desired place of other files. In this thesis the `sed` and `awk` commands are used to put the basic parameters file in the input files and the pseudopotentials file in the file .files.

2.3 Convergence of principal parameters

As it was explained in the introduction chapter, the calculation of the quasiparticle energies requires of previous convergence studies over certain parameters. One of these parameters is the energy cut for ground state energy, dynamical screening W, and the self-energy Σ; the other one is the number of bands for dynamical screening and for the self-energy. The energy cut is related to the Fourier's components of the discrete Fourier transform involved in the representation of charge density, wave functions, dynamical screeening and the self-energy in the reciprocal space. The different summations over the **G** vectors that appear in equations 1.9, 1.30 and 1.34 define the energy cut in the form

$$E_{cut} = \frac{|\mathbf{k} + \mathbf{G}|^2}{2} \tag{2.1}$$

where **k** are the k vectors within the IBZ and **G** are the vectors in reciprocal space of the plane-waves expansion. The convergence for the number of bands comes from the summations over states in equations 1.30 and 1.34.

   The convergence test of the energy cut of the ground state consists in changing the value of the energy cut, until the total energy of the crystalline system reaches a stable value. With the charge density computed in this step is possible to obtained the Kohn-Sham wave functions that are needed to calculate the dynamical screening and the self-energy. The convergence test of the energy cut of the dynamical screening, and the self-energy is done with the convergence of the quasiparticle energy for a specific k-point (for instance the Γ point), and a specific energy band. In this context the convergence of the energy cut for dynamical screening requires the calculation of the quasiparticle energy, by means of the calculation of the self-energy as in equations 1.34 and 1.29. Thus, the polarizability 1.30 is computed in order to calculate the dynamical screening for each value of energy cu,t and after that, the quasiparticle energy is computed with equations 1.29 and 1.34. A converged value of this energy is the stop point of the convergence test for dynamical screening. The energy cut of the self-energy uses the screening computed in the previous convergence test, and also reaches a stable value of the quasiparticle energy for a specific k-point and band. The convergence over number of bands is also achieved with the same protocol used for the convergence of energy cut: the dynamical screening and the self-energy are computed by changing the number of bands

until the quasiparticle energy is converged.

In the Abinit code the calculation of the quasiparticle energies can be done in a one-shot run that is divided in four steps. The first step computes the charge density with SFC method for a specific energy cut. The second one computes the Kohn-Sham wave functions with the charge density calculated in the previous step. The third step calculates the dynamical screening taking the wave functions of the second step. And the fourth step computes the quasiparticle energy using the dynamical screening and wave functions of previous steps. Good results for quasiparticle energies are achieved if the energy cut and number of bands are converged. In this work the calculation of the quasiparticle energies for different k-points is done with separate calculation of the four steps. The different parameters are inherited in order to obtain better results of each one of the convergence test.

An example of convergence of one of the parameters, the energy cut (ecut), is illustrated in the figure 2.2. An initial value of the parameter is introduced in the Abinit input file; the total energy of the system found is saved for evaluating the tolerance criterion. The ecut is augmented in a certain integer step and the total energy is evaluated again. This new total energy is compared with the previous one to verify if the tolerance criterion is accomplished. In case that the criterion is not achieved the ecut is augmented and a new Abinit run starts. The bucle will finish when the total energy converges under the tolerance criterion selected.

Others parameters are converged in the same way. Number of bands and ecut for screening and self-energy are increased until the tolerance criteria are obtained. In this case, wave functions are used for calculating the screening and this is used to compute the self-energy and the quasiparticle energy. The tolerance criterion is evaluated, based on energy of a specific point and a specific band. Figure 2.3 illustrates schematically the convergence study for number of bands (nband) of self-energy. All these convergence tests were coded with a bash script. An example of one script is shown in the appendix for the convergence of the energy cut.

The edition of the files used for the Abinit runs is done with the *sed* command. This allows to change the value of the ecut or nband parameters for convergence. The *grep* command is used for extracting the values of total energy and quasipaticle energy of output files in order to evaluate convergence criterion. The operations to evaluate the tolerance criterion are written in *bash* language.

2.4   Calculation of the screening, self-energy and quasiparticle energies

Once all parameters are converged the calculation of the screening and self-energy for computing the quasiparticle energies can be done. In this case the GW correction is applied to all bands of all k-points generated by a homogeneous grid in the IBZ. The number of k-points must be enough for a converged calculation of the dielectric function. The screening and self-energy are calculated with the converged values of energy cut and number of bands of the previous section. This computation
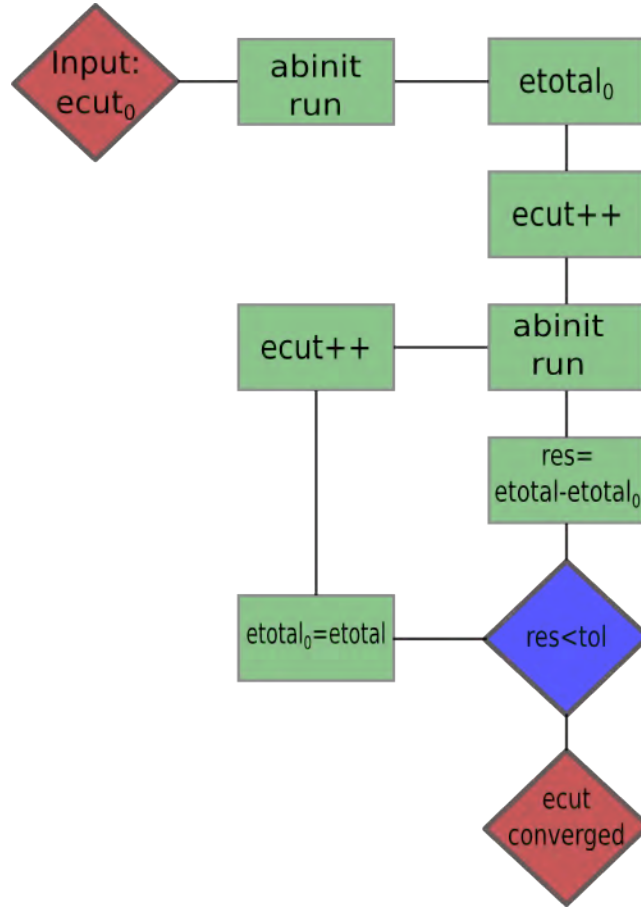
Figure 2.2: Convergence of the variable energy cut (ecut)

is done with the same number of k-points for both screening and self-energy. Dielectric function of most semiconductors materials achieves convergence with a grid of $20 \times 20 \times 20$ that is equivalent to 256 k-points. However, for metallic materials is necessary to choose a more dense k-point grid. The list of k-points is generated with Abinit and later these k-points in the IBZ are included in the input files of screening and self-energy. The computation of screening is done and the file with matrix element of screening are used for calculating the self-energy and so the quasiparticle energies. The bands and the number of bands chosen for the calculation depends principally of the bands involved in the optical absorption, for instance the Si requires 12 bands for a complete description of the band gap and dielectric function.

The energy for each k-point and each band are concatenated in a text file by extracting the relevant information of quasiparticle energies from the Abinit output files. A fragment of the code where the quasiparticle energies are extracted of the output files is shown in the appendix. A python script where the quasiparticle energies are organized in another text file is also shown in
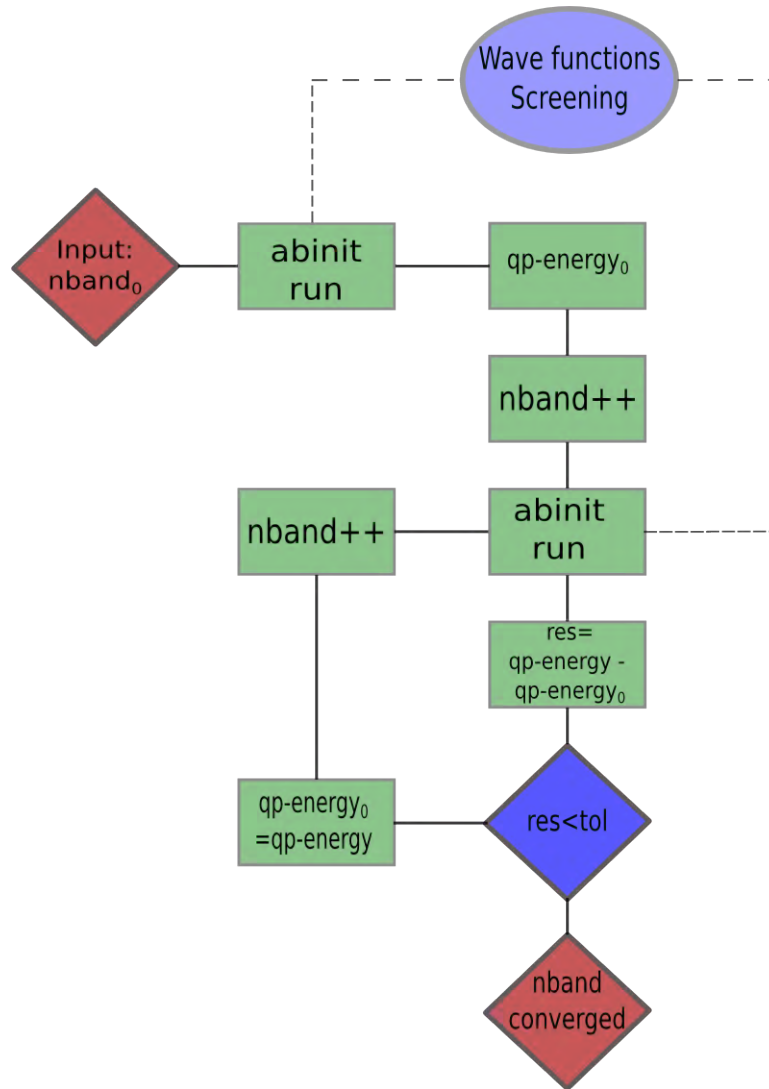
Figure 2.3: Convergence of the number of bands for self-energy

the appendix. After the manipulation of the files that contain the important information, a file with name `bndGW-n_kpt-Sys` is created to contain the values of the quasiparticle energies for all k-points and band energies. Also, in the code of the automated program the energy bands are calculated for the same k-points that are included in a text file with name `bndDFT-n_kpt-Sys`. Thus, it is possible to plot both DFT-LDA energies and GW quasiparticle energies for comparisons. `bndDFT-n_kpt-Sys` and `bndGW-n_kpt-Sys` are added to the directory with name `Sys-grid-n_kpt` that are created automatically when the `GW.sh` script are executed. Besides, at the end of the calculation there is a directory that includes: a text file with the values of the converged parameters, a text file with band gap information, a file with the list of k-points used, different plots of band

energies of the k-points, band structure with an average correction and band structure with scissor correction. In the case of metallic systems a file with information about Fermi energy and a plot with spectral function of the system are added to the directory of the results.

2.5 Band structure of semiconductors and spectral function of metals

2.5.1 Band Structure

The calculation of the GW correction for high symmetry k-points is not possible in Abinit because these points present a special difficulty. These high symmetry points are present in different regions of the Brillouin Zone. For this reason the application of the symmetry matrices of the system is not be able to reduce to a minimum the high symmetry k-points. The method that Abinit uses for the generation of k-points is the Monkhorst-Pack method [46]. This procedure generates k-points in the middle of the IBZ and does not produce k-points in the limits. However the calculation of the quasiparticle energies of several k-points for semiconductors allows to compute an average value of the correction on energy for each energy band taking into account all k-points. A calculation of the average correction to energy with the GW approximation over each band, allows to compute the electronic band structure of semiconductors. The expression for the calculation of the average of the correction on energy is given by

$$\overline{E}_n = \frac{\sum_k^{IBZ}(E_{n\mathbf{k}}^{GW} - E_{n\mathbf{k}}^{LDA})}{N_k},\qquad(2.2)$$

where $\overline{E}_n$ is the average value of the energy corrections in the nth band, E_n^{GW} is the quasiparticle energy computed with the GW approximation and E_n^{LDA} is the energy computed with LDA approximation for the same band n. N_k is the total number of k-points used for the calculation of the energy bands. Thus, the band structure of the system is calculated using LDA approximation and these energy bands are corrected with the values of the energies computed with the expression 2.2.

2.5.2 Spectral function

The quasiparticle energies also provide a good calculation of the spectral function of metals. This function provides information about electronic transition and collective excitations like plasma excitations. Spectral function also provides a good comparison with experiments via photo emission spectroscopy (PES). Using the self-energy operator $\Sigma(\omega)$ in the frequency space and the LDA eigen-energies the quasiparticle and plasmon satellites peaks can be computed with the expression [47]

$$\langle\phi_{n\mathbf{k}}|A(\omega)|\phi_{n'\mathbf{k}}\rangle = \frac{|\mathrm{Im}\,\langle\phi_{n\mathbf{k}}|\Sigma(\omega)|\phi_{n'\mathbf{k}}\rangle\,|}{[\omega - E_n(\mathbf{k}) - \mathrm{Re}\,\langle\phi_{n\mathbf{k}}|\Sigma(\omega)|\phi_{n'\mathbf{k}}\rangle]^2 + [\mathrm{Im}\,\langle\phi_{n\mathbf{k}}|\Sigma(\omega)|\phi_{n'\mathbf{k}}\rangle]^2},\qquad(2.3)$$

where $\Sigma(\omega)$ is the self-energy and $E_n(\mathbf{k})$ are the eigen-energies of the system. In Abinit the numerical calculation of the spectral function $A(\omega)$ is done with the equation 2.3; taking $E_n(\mathbf{k})$ energies as the

quasiparticle energies $E_n^{QP}(\mathbf{k})$ calculated with the GW approximation, and taking wave functions $\phi_{n\mathbf{k}}$ as the Kohn-Sham wave functions. An output file with extension *SIG* that contains the value of $A(\omega)$ in a given interval of frequencies is generated when the GW approximation is used to get quasiparticle energies of metals.

2.6 Calculation of linear dielectric function with *TINIBA*

In this thesis the calculation of the linear dielectric function using quasiparticle energies is not automatized. However, this calculation is done using the TINIBA code. This code is used by the group of Propiedades ópticas de interfases, superficies y metamateriales of the Centro de Investigaciones en Óptica, for the different researches related to optical properties of matter from a computational point of view. This open source code is available online and is registered in the Instituto Nacional de Derechos de Autor (INDAUTORMéxico) with the register number 03-2009-120114033400-01 [45]. TINIBA is a program focused in the calculation of optical properties of bulk and surface systems. Important functions like linear and non-linear dielectric function, spin injection and current injection can be computed by TINIBA. The quasiparticle energies calculated in the previous section allow to compute the linear dielectric function with RPA approximation using the equation 1.30. The computation of the linear dielectric function is done with the TINIBA code and only requires the calculation of wave functions and momentum matrix elements $M_G^{n,n'}(\mathbf{k}, \mathbf{q})$ which can also be computed by TINIBA. This part of the calculation is not automatized but it can be done easily with TINIBA code following the basic steps of a tutorial available online. In this work the linear dielectric function of different semiconductors was calculated with Kohn-Sham eigen-energies in LDA approximation and with the quasiparticle energies obtained with the GW approximation using the automated program. The complete procedure of this thesis is summarized in the figure 2.4: starting with convergence parameters (ecut, ecuteps, ecutsig, nband, etc.), continuing with the calculation of screening W, self-energy Σ and quasiparticle energies and finally with the calculation of the linear dielectric function.
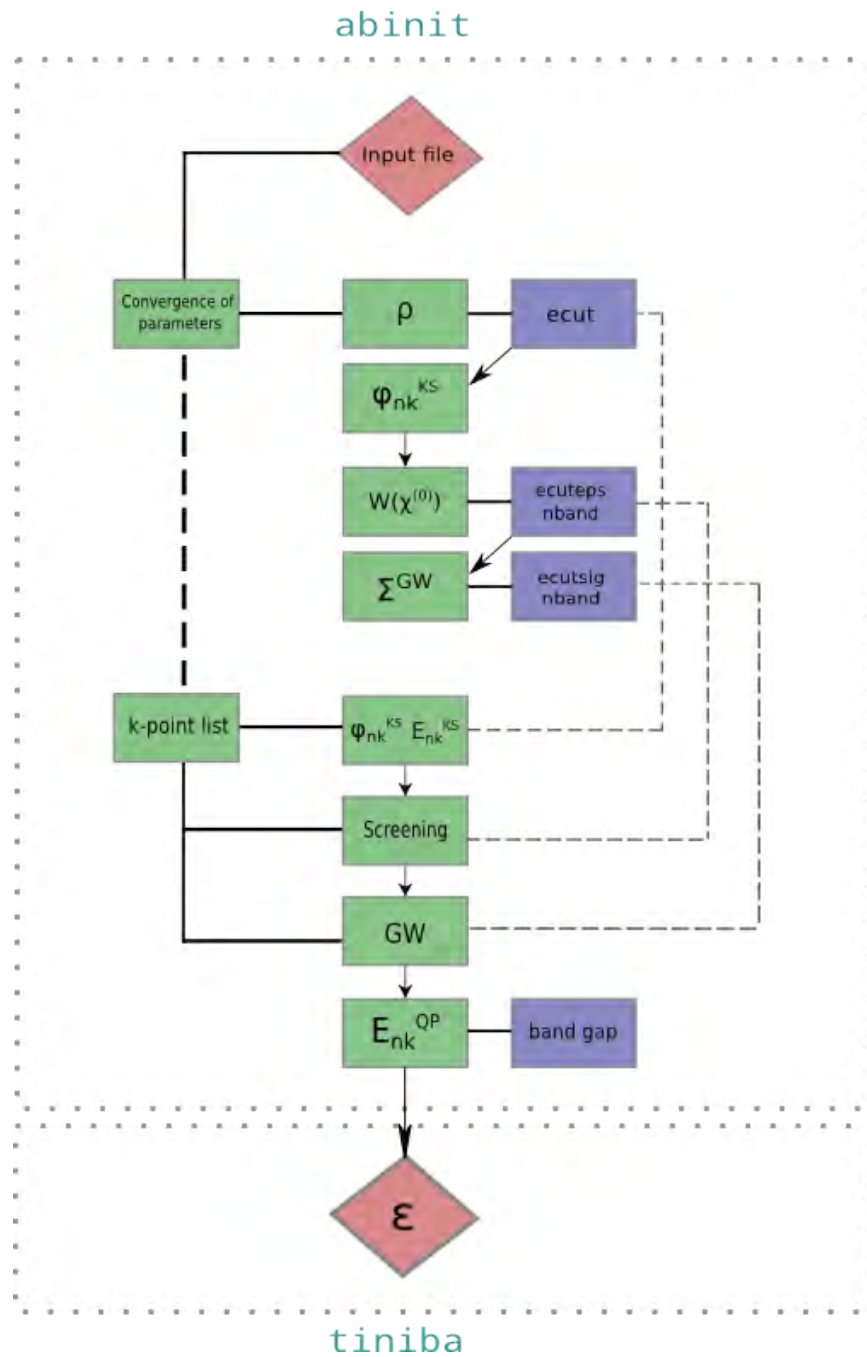
Figure 2.4: Summary of the total procedure for the calculation of linear dielectric function with quasiparticle energies

3 RESULTS

Outline

In this chapter are shown the results of the automated program, that allowed to compute energy bands and quasiparticle energies of three semiconductors and three metals. In this chapter are also shown the results of optical band gaps for semiconductors, Fermi energies and the spectral function of metals. Finally, we shown the results of the linear dielectric function, computed with TINIBA, for the same semiconductors and metals.

3.1   Energy bands

In the Abinit code is not possible to compute the quasiparticle energies for high symmetry points. This is due to the fact that high symmetry points can belong to different regions of the Brillouin Zone; thus the symmetry operations (symmetry matrices that are applied over **k** vectors) are inefficient at the moment of distinguishing points of one IBZ of another one. Hence Abinit does not allow the calculation of the GW correction for those k-points. However, the results obtained for quasiparticle energies of k-points within IBZ of semiconductors allow to conclude that the energies computed with LDA approximation of a specific band are corrected in an average numerical value for most k-points. This results of the average of energies are used as an approximation to correct rigidly the value of each energy band of the electronic band structure. Specifically, an average value of the GW correction is obtained using the quasiparticle energies of several k-points within IBZ of a specific energy band; and the result of that average value is used to correct the same energy band of the electronic band structure computed with LDA approximation. The average values were computed in this work with a basic python script using the expression 2.2.

3.1.1 k-points inside of the IBZ

The method implemented in Abinit for the generation of the k-points is the Monkhorst-Pack method [46]. This method generates an homogeneous grid of k-points in the Brillouin Zone. In this work the size of the grid generated by the Monkhorst-Pack was of $20 \times 20 \times 20$ for the full Brillouin Zone, which is equivalent to 8000 k-points. The application of the symmetry operations reduces to 256 the number of k-points in the IBZ. This quantity of k-points are enough to compute the linear dielectric function of semiconductors with a high convergence.

The results obtained for energy bands of k-points within the IBZ of the semiconductors Si, GaAs and Ge are shown in the figures 3.1 3.2 3.3. The continuous lines represent the results obtained with LDA approximation, black points represent the GW correction to energy of the same k-points. Blue continuous lines represents the LDA eigen-energies of conduction bands and red continuous lines represents the valence bands of same crystalline system. The plots show that the correction on energy have a certain average value for some energy bands. Thus, it is possible to observe that for Si the conduction bands do not present an appreciable correction on energy while the valence bands are corrected by the values shown in the figure 3.1. It is also possible to observe that the correction on energy of the first valence band is different of the correction on energy of the other bands. This difference on the correction on energy can be notably appreciated between the first and fourth valence band. Another point to note is that the fourth band has been corrected by a higher average value than the other valence bands. Finally, the results allow to conclude that k-points near of G point have the minimum correction with respect to other points of the same energy band; all the energies of the first k-point in the plots belongs to G point and the next ones are points near of G point. Similar results were obtained for Ge and GaAs. In these systems all the valence bands have been corrected. Furthermore, as in the Si system each energy band was corrected by different values; it can observed that the correction of the fourth band is greater than the correction of the other valence bands. On the other hand the conduction bands remain practically equal. For all these semiconductor were found that the energy of the valence bands decreases with the GW approximation being the correction higher for the last valence band. The calculation of the quasiparticle energies for all these systems required an average computational time consuming of six days using 64 cores for each system.

In the case of metallic systems we can observe that the behavior of the correction on energy for each k-point is totally different respect to the semiconductor systems. For Cu, Au and Ag in the figures 3.5 3.6 3.4 it is possible to appreciate the correction on energy of these systems. Unlike the results obtained for semiconductors, the correction on energy for each k-point varies substantially for each k-point: some energies increase and others decrease. The results show that for the same band energy, there are energies that do not present corrections while other points present corrections on energy that even exceed the energies calculated with LDA for other energy bands. Furthermore, the energies of the conduction bands are corrected. Hence, for metallic systems all bands are corrected. These results prevent to correct the band structure of metals using the expression 2.2 because the correction on energies for each energy band does not have a certain average value like semiconductors. However, the quasiparticle energies obtained are enough to compute the linear

Figure 3.1: Energy bands of Si for a 256 k-point inside of the IBZ. Red lines: valence bands. Blue lines: conduction bands. Black points: quasiparticle energies.

Figure 3.2: Energy bands of GaAs for a 256 k-point inside of the IBZ. Red lines: valence bands. Blue lines: conduction bands. Black points: quasiparticle energies.
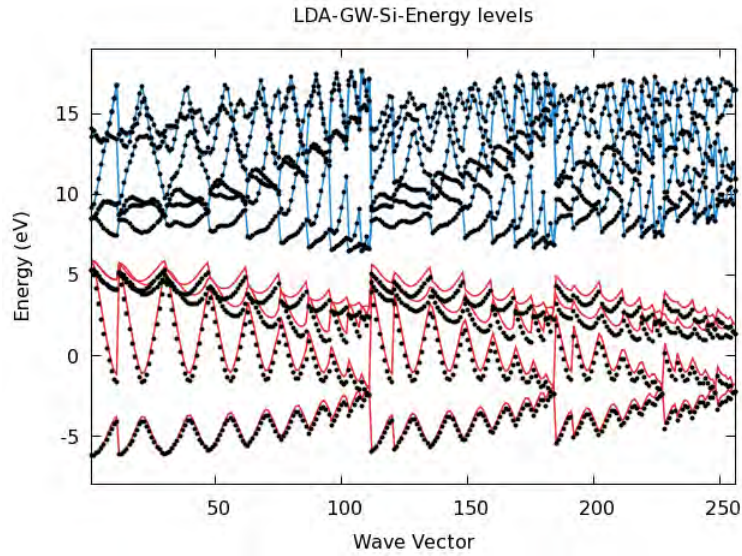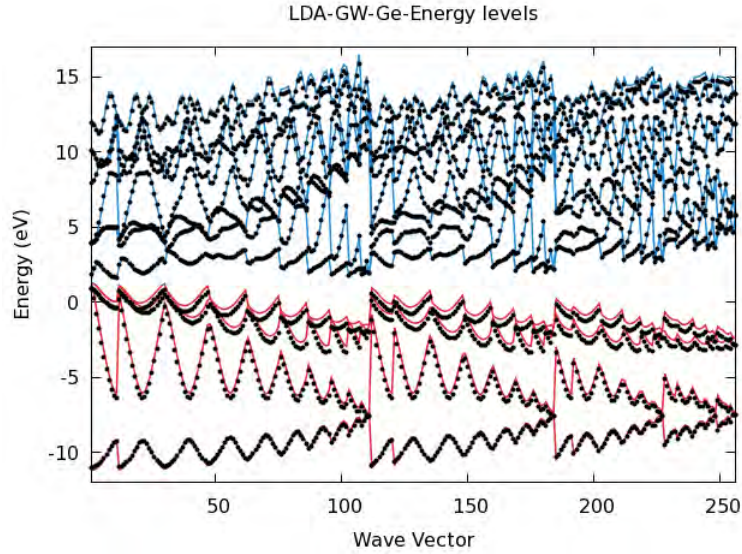
Figure 3.3: Energy bands of Ge for a 256 k-point inside of the IBZ. Red lines: valence bands. Blue lines: conduction bands. Black points: quasiparticle energies.

dielectric function of metals. Furthermore, in all these cases the Fermi energy (black line for Fermi energy computed with LDA and red line for Fermi energy computed with GW approximation) changes around 2 eV for Ag an Au, and 4 eV for Cu. In the case of metals, the computation time was around three days.

Figure 3.4: Energy bands of Ag for a 256 k-point inside of the IBZ. Red lines: valence bands. Blue lines: conduction bands. Black points: quasiparticle energies.
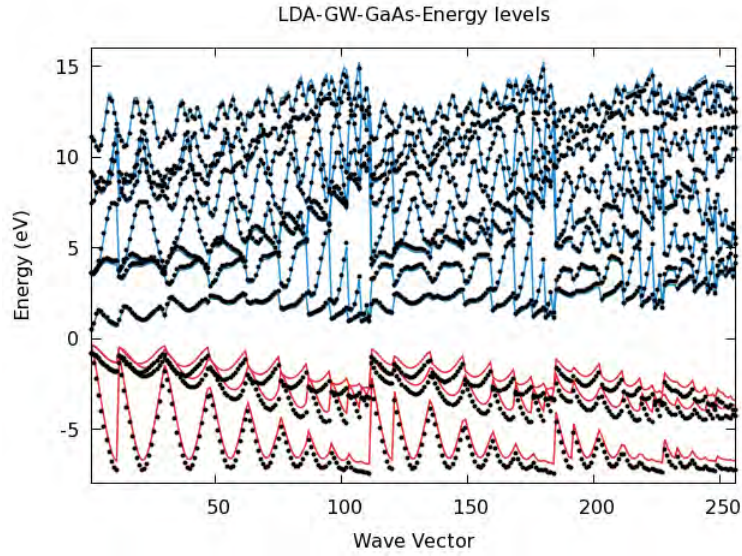

Figure 3.5: Energy bands of Cu for a 256 k-point inside of the IBZ. Red lines: valence bands. Blue lines: conduction bands. Black points: quasiparticle energies.

Figure 3.6: Energy bands of Au for a 256 k-point inside of the IBZ. Red lines: valence bands. Blue lines: conduction bands. Black points: quasiparticle energies.
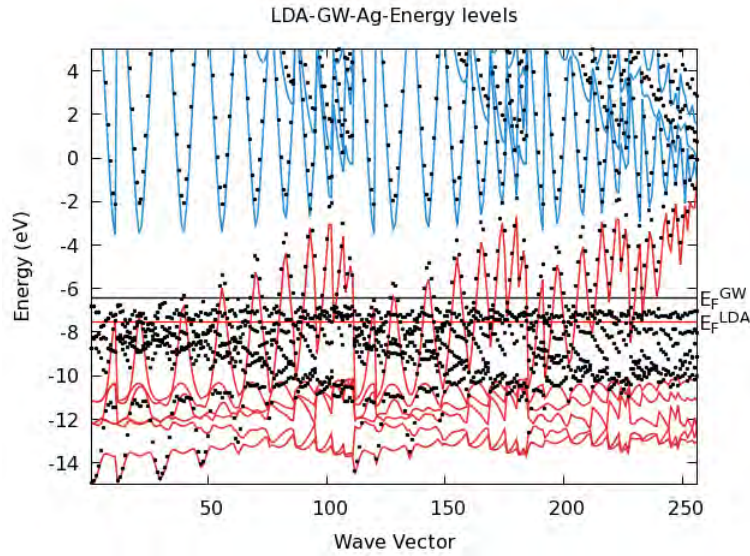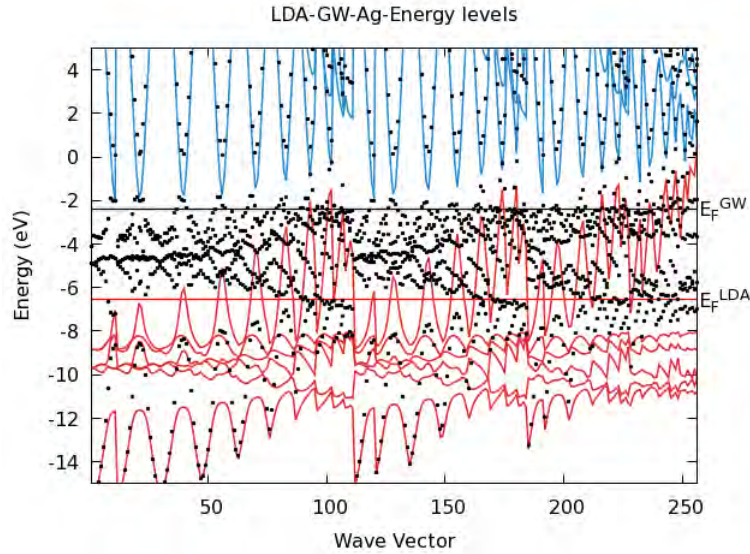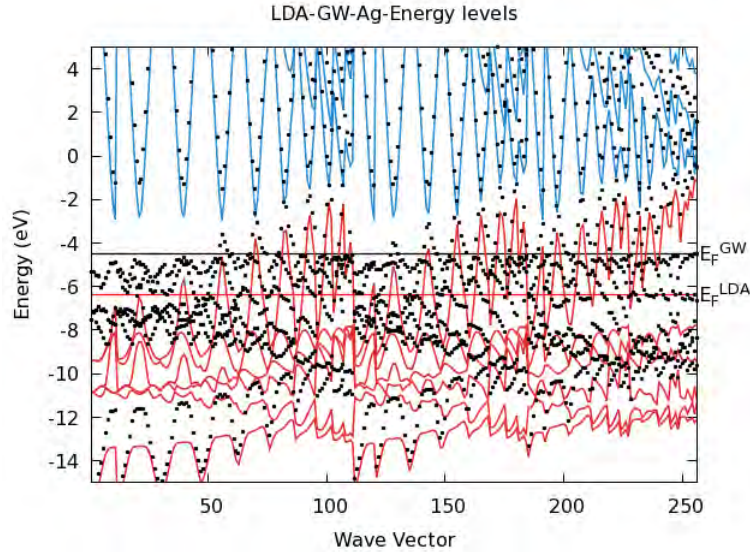
3.1.2 Band structure

A calculation of the average correction on energy with quasiparticle energies over each band, allows to do an approximation of the electronic band structure of semiconductors. Although it is better to calculate directly the quasiparticle energies of the high symmetry k-points, in the previous chapter was mentioned that Abinit does not allow to compute them. However, this approximation is good due to the linear average correction of each band with the GW approximation. In this case the average of the correction on energy is calculated with the expression 2.2. Displacing rigidly each band of energy calculated with LDA approximation (for high symmetry k-points) by the average value given by 2.2 the plots 3.7 3.8 3.9 are obtained.

The results allow to get for semiconductors a more accurate optical band gap than the computed with LDA for the systems evaluated [13,14]. It is also possible to observe the same results commented in the case of quasiparticle energies of k-points inside of the IBZ: valence bands presents correction on energy while conduction bands do not; the fourth valence band present a higher correction on energy than the first valence band.

Figure 3.7: Electronic band structure of Si with LDA and GW approximation. Red lines: valence bands. Blue lines: conduction bands. Black points: quasi-particle energies.

Figure 3.8: Electronic band structure of GaAs with LDA and GW approximation. Red lines: valence bands. Blue lines: conduction bands. Black points: quasiparticle energies.
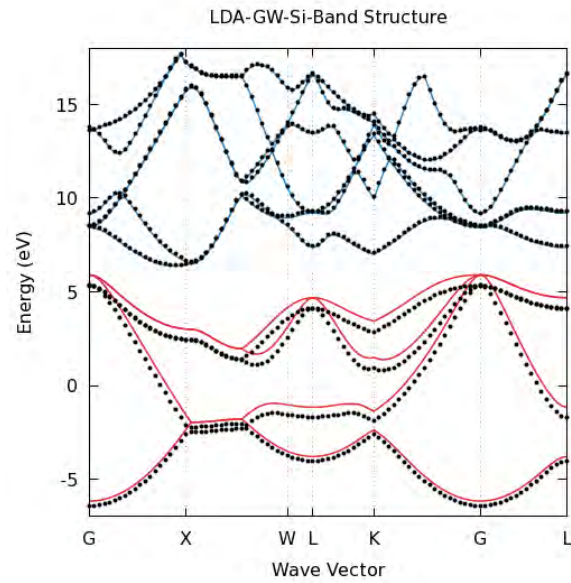
Figure 3.9: Electronic band structure of Ge with LDA and GW approximation. Red lines: valence bands. Blue lines: conduction bands. Black points: quasiparticle energies.
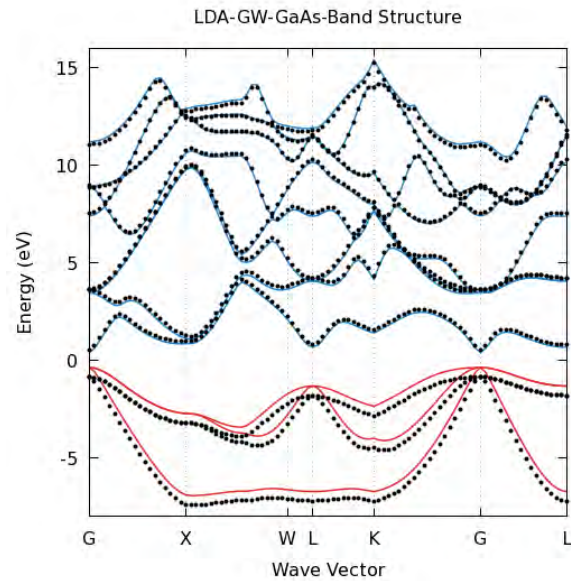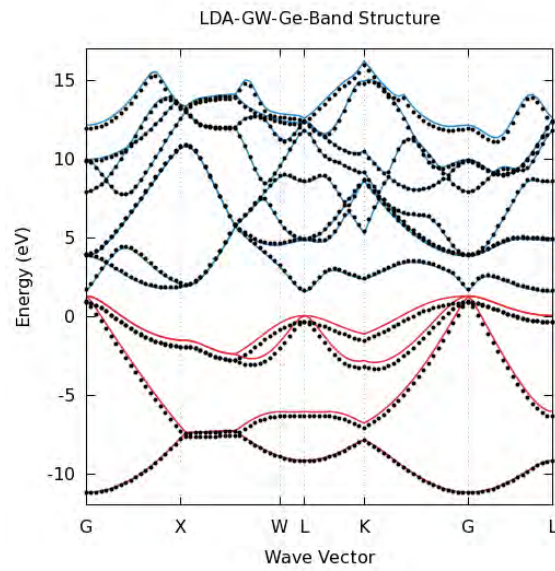
3.2 Spectral function

In the case of metallic systems, the calculation of the quasiparticle energies provide a good accuracy for the calculation of the spectral function $A(\omega)$ with the expression 2.3. For each k-point there is a spectral function. The results of the spectral function of Au, Cu and Ag are shown in the figures 3.10 3.11 3.12. This calculation were done for the Gamma point.
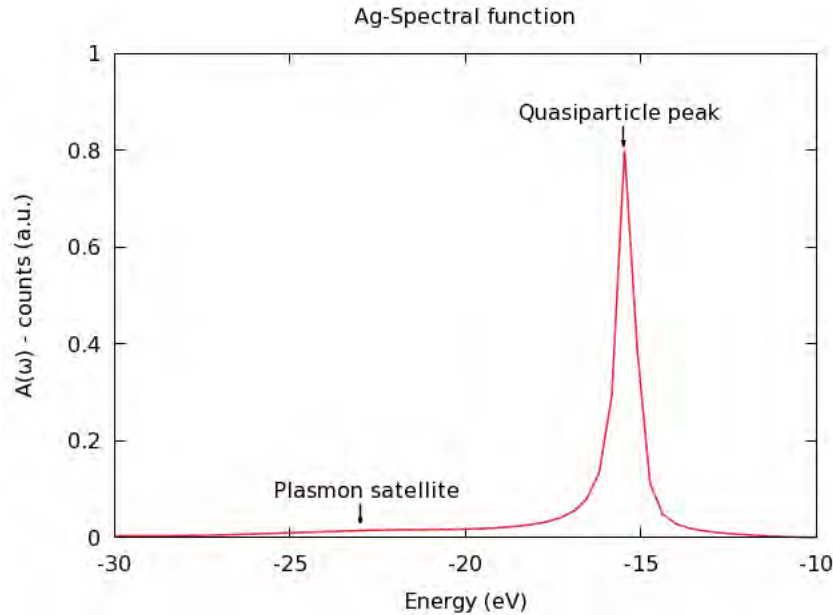
Figure 3.10: Spectral function of Ag computed with quasiparticle energies

The results show quasiparticle peaks for energies near of -15 eV for Au, Cu and Ag. This energy corresponds to the energy of the bottom of the first valence band as it can be observed from energy bands of figures 3.4 , 3.5 and 3.6. Plasmon satellite peaks are also included. Plasmon eneries of -27 eV, -31 eV and -23 eV were found for Ag, Cu and Au respectively. In all these cases the quasiparticle peak has a greater value of $A(\omega)$ than the plasmon peak, due to the fact that the electronic transitions present the major contribution to external perturbation, in comparison with the resonance between electromagnetic incident waves and plasmons. In the case of Cu another peak is found between the plasmon energy and quasiparticle energy because the plasmons oscillations can absorb energy of the quasiparticle excitations and contribute with some additional peaks.
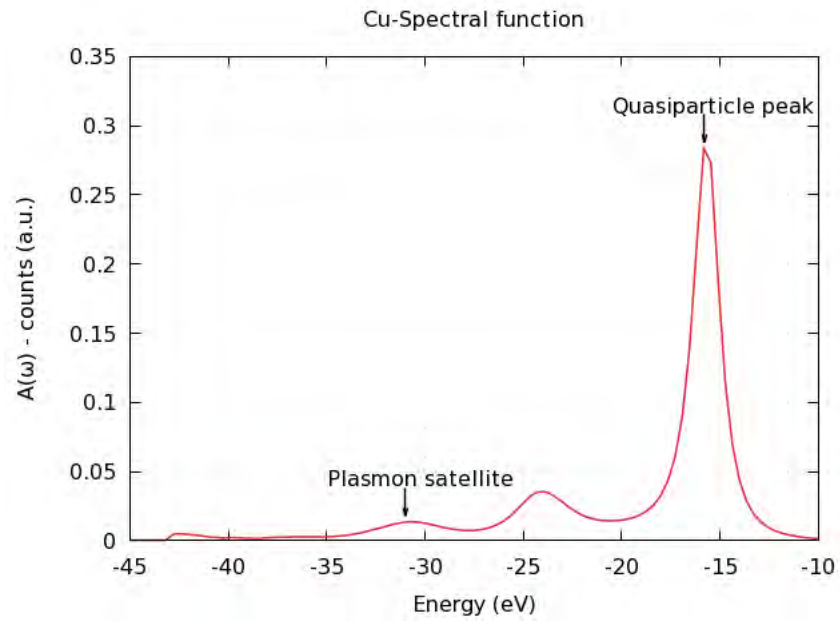
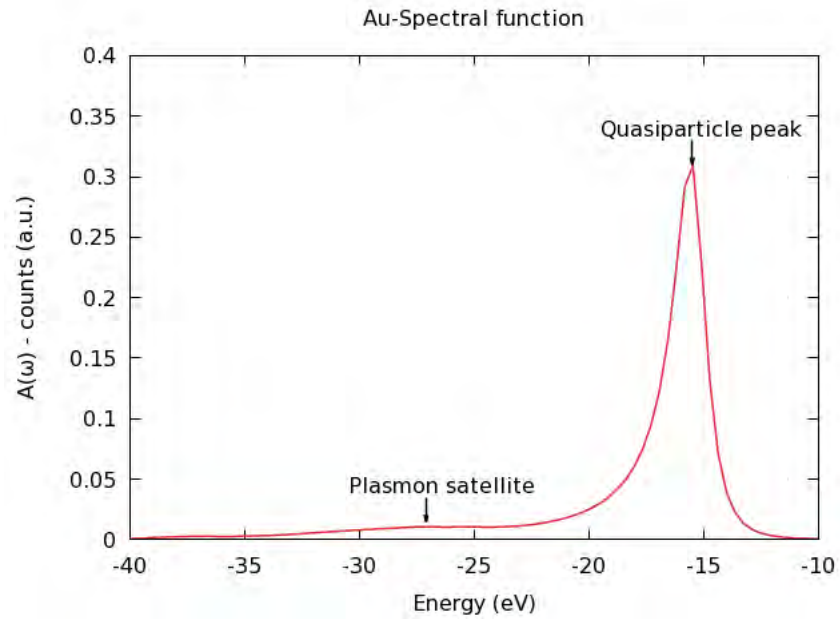Figure 3.11: Spectral function of Cu computed with quasiparticle energies

Figure 3.12: Spectral function of Au computed with quasiparticle energies

3.3 Optical band gap and Fermi energy

The quasiparticle energies computed with the GW approximation allow to acquire a more accurate band gap and Fermi energy than the band gap and Fermi energies obtained with the LDA approximation. The results obtained for electronic affinity and ionization potential from MBPT and GW approximation gives an optical band gap with an error below 10% respect to experiments [42, 48, 49]. Fermi energies acquired with quasiparticle energies also present different results in comparison with results computed with LDA eigen-energies [50, 51]. Experimental Fermi energy results are not shown because the zero energy reference may be different between different experiments. The tables 3.1 and 3.2 summarizes the optical band gap values and Fermi energies computed with quasiparticle energies.

Optical band gap (eV)				
System	LDA	GW	$E^{GW} - E^{LDA}$	EXP [48]
Si	2.530	3.205	0.676	3.40
GaAs	0.725	1.315	0.590	1.42
Ge	0.356	0.997	0.641	0.89

Table 3.1: Energies of the optical band gap calculated in the point k(0,0,0), with LDA and GW approximations

Fermi energy (eV)		
System	LDA	GW
Ag	-7.55	-6.44
Cu	-6.56	-2.38
Au	-6.36	-4.49

Table 3.2: Energies of the Fermi level calculated with LDA and GW approximations

3.4 Dielectric function

The results obtained for the imaginary part of the linear dielectric function ϵ_2 of the Si, GaAs and Ge are shown in the figures 3.13 3.14 3.15. The plots show the results obtained with LDA approximation, GW approximation and experimental results [52, 53]. It is possible to observe that the position of the peaks E_1 and E_2 computed with LDA are totally different of the position of the same peaks computed with GW approximation. In the last case, the linear dielectric function computed with quasiparticle energies is more similar to the experimental results. It can also be appreciated that the range of absorption of the ϵ_2 calculated with quasiparticle energies is near to the experimental

one. The results obtained with LDA approximation do not coincides with experiments neither in absorption range nor in intensity. The optical band gap (where ϵ_2 acquires values different of zero) computed with GW approximation also is in a good agreement with experiments [52,53]. This result coincides with the values calculated with GW approximation for optical band gaps shown in the table 3.1. Two principal peaks E_1 and E_2 can be observed in the plots. The peak E_1 is related to electronic transition between the fourth valence band and the first conduction band. This explains the correspondence between the optical band gap energy and the energy of the peak E_1. The peak E_2 is given by the electronic transitions between valence and conduction bands that correspond to the energy of the peak E_2.

Figure 3.13: Imaginary part of the linear dielectric function of Si computed with quasiparticle energies and LDA energies

In the case of Si, one peak of absorption near of 4.5 eV were obtained with the GW approximation. This peak is aproximated in frequency and intensity with experiments while the peak of absorption with LDA approximation are present in a frequency is near of 3.7 eV. The results also show a peak near of 3 eV with the GW calculation but that peak dose not achieve the intensity that appeared in the experimental results. This peak of absorption in the experiments is consequence of the excitonic effects which the GW approximation does not have into account. A better calculation of the linear dielectric function with excitonic effects must include a two-particle Green's function. Thus, the interaction between holes and electrons allow to obtained a linear dielectric function with a better approximation regarding with experiments. However, the results obtained in this work contains relevant information about optical band gaps, intensity of the quasiparticle peak of absorption and absorption range of frequency.

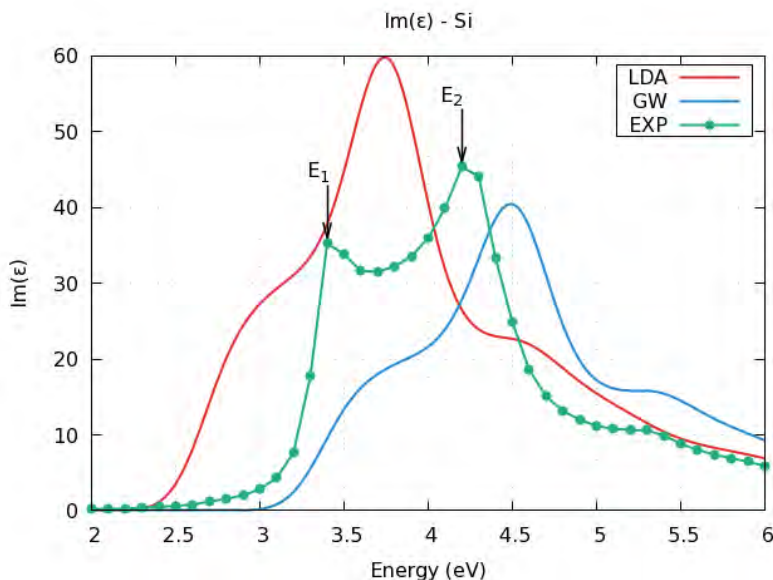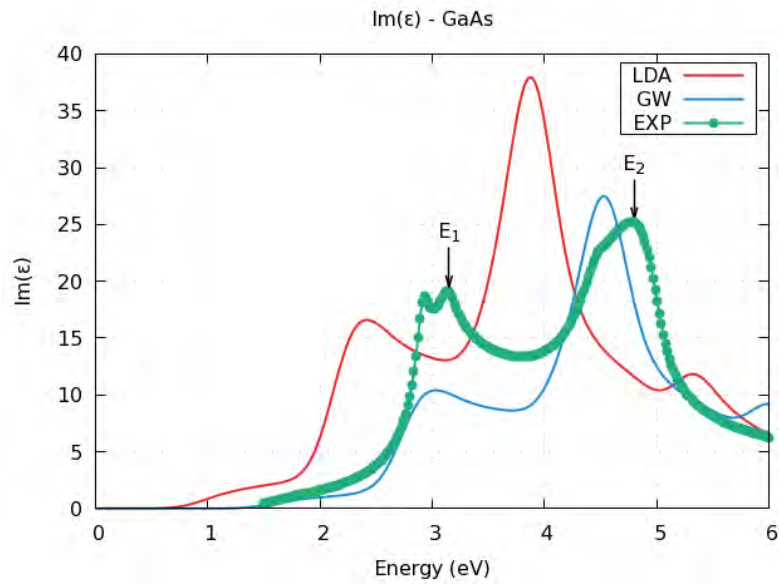Figure 3.14: Imaginary part of the linear dielectric function of GaAs computed with quasiparticle energies and LDA energies
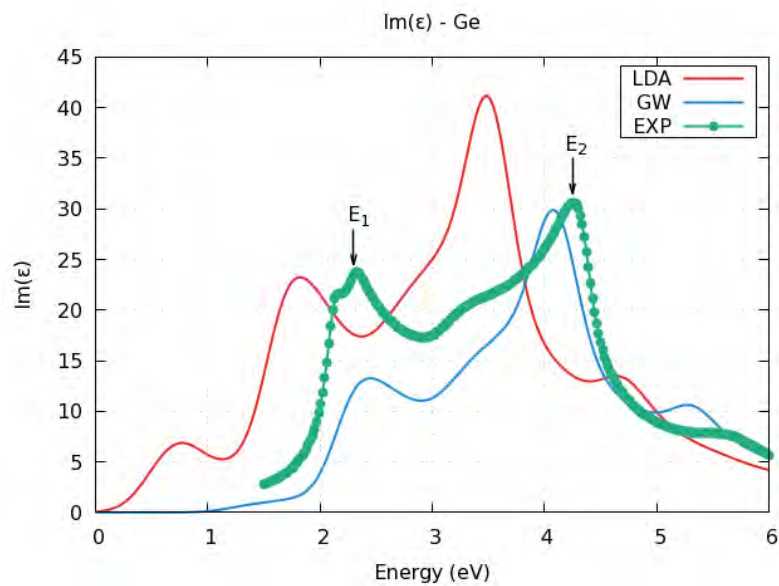

Figure 3.15: Imaginary part of the linear dielectric function of Ge computed with quasiparticle energies and LDA energies

For GaAs and Ge similar results were obtained. The imaginary part of the linear dielectric function computed with LDA approximation is very different from that computed with GW approximation. In the case of GaAs there are two peaks near of 3 eV and 4.5 eV. For Ge there are two peaks near of 2.5 eV and 4 eV. It is also possible to observe a peak of absorption in the LDA approximation near of 0.7 eV. This peak disappears in the GW approximation. Again, a complete description of the imaginary part requires the calculation of the eigen-energies with excitonic effects to achieve the intensity of the first peak.

In the case of metallic systems different results are obtained. The results are shown in the figures 3.16, 3.17 and 3.18. In this case the imaginary part of the linear dielectric function of Ag, Cu and Au, computed with quasiparticle energies, does not approximate to the experimental results in comparison with the results obtained with LDA energies. The results obtained with LDA are better than those obtained with GW approximation respect to experiments [54, 55]. It is possible to observe from experimental results that the energy transitions begin around 4 eV. With LDA approximation electronic transitions start around 2 eV and with GW approximation start near of 0 eV. This last result is not compatible with experimental results. As it was mentioned in the case of the energy bands for metals, the GW correction for metals is not trivial. Energy bands are not corrected rigidly as in the case of semiconductor systems. For this reason, the GW correction for metals requires of a more detail work. One of the alternative that was taken into account was the type of smearing for integration. The calculation of the different physical properties requires an integration over k-points. This integration requires of a smearing function around Fermi energy because at this energy there is a discontinuity. Different smearing function were used for the calculation of the quasiparticle energies. Gaussian, Fermi-Dirac and polinomial approximation (known as cold smearing) were used. With these energies the linear dielectric function of Ag was computed. Although it is possible to observe different results in figure 3.16, those results are not approximated to experimental results. One of the possibilities to achieve better results is to use another smearing functions, or to work directly with the pseudopotentials. It is possible that core electrons contribute significantly to valence energy bands. In this case the pseudopotentials must be changed but that work escapes of the principal objective of this thesis. In conclusion, better results for metals could achieve but with a more detail investigation.
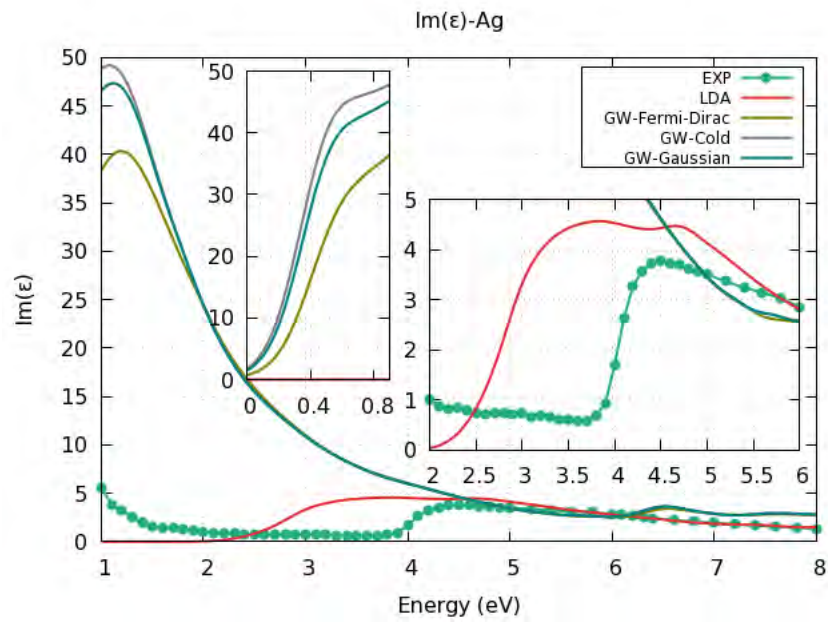
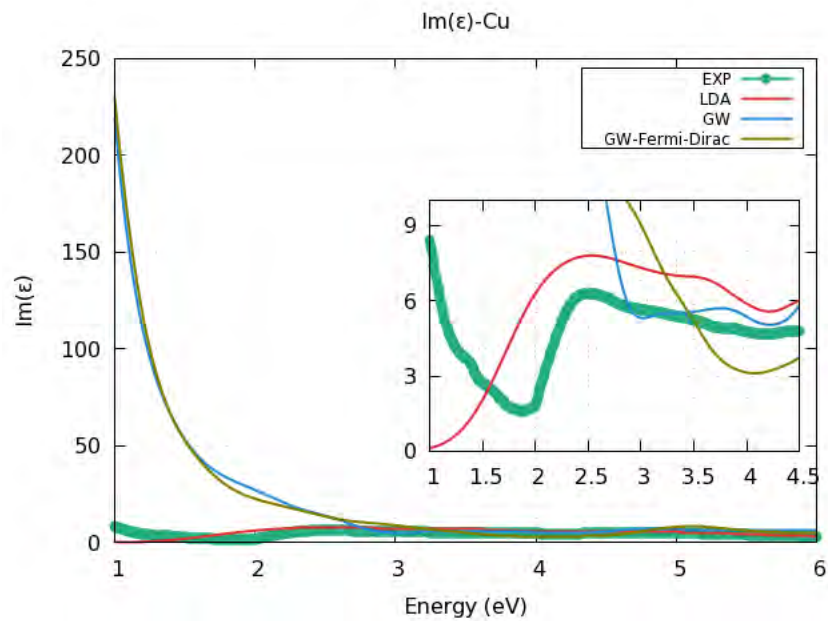Figure 3.16: Imaginary part of the linear dielectric function of Ag computed with quasiparicle energies

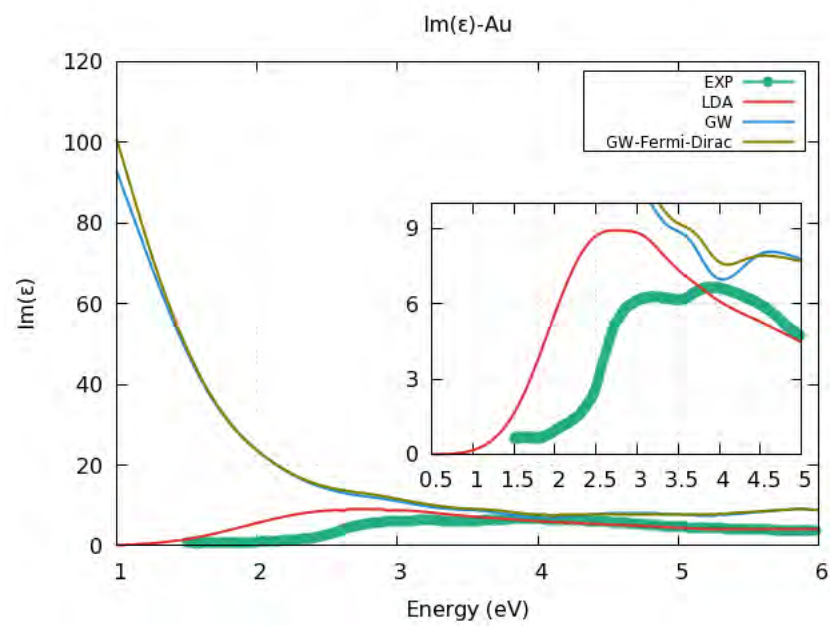Figure 3.17: Imaginary part of the linear dielectric function of Cu computed with quasiparicle energies

Figure 3.18: Imaginary part of the linear dielectric function of Au computed with quasiparicle energies

4 CONCLUSIONS

- The program developed in this thesis calculates, without technical problems, the eigen-energies with LDA approximation and quasiparticle energies with GW approximation for semiconductors. The program also computed the optical band gap of semiconductors.

- The program calculates the quasiparticle energies and LDA energies of metals, but the type of smearing used provides different results. The program also computes the Fermi level and spectral function of metals.

- The automated program is able to calculate the quasiparticle energies, optical band gap, Fermi level and spectral function of other crystalline systems for future optical researches of semiconductors and metals.

- The optical band gap calculated with GW approximation is better than the results obtained with LDA approximation respect to experimental results.

- The electronic band structure of the semiconductors calculated with GW approximation is better than the results obtained with LDA approximation.

- The linear dielectric function calculated with quasiparticle energies is better than the calculated with LDA approximation respect to experiments.

- A better calculation of the liner dielectric function for semiconductors demands the use of the Bethe-Salpeter equation where excitonic effects are present.

- The linear dielectric function of metals computed with quasiparticle energies does not approximated to experimental results. The GW study of metals requires of a more detail investigation.

A Bash script for the convergence of the energy cut

```
#these parameters are inherited by another script
tol=$1
cores=$2
brav=$3
ecutfound=0
iecut=3.0
int=1.0


#Program to compute the principal ecut
cd ecut2/  #directory where the convergence test is evaluated

#erasing files of previous calculations
rm -f ecut2.in ecut2.out mecut2.in mecut2.out ecut_dat
cp pre_ecut2.in ecut2.in

#adding global parameters to input file
sed -i '/#general_parameters/ r general_param.cdl' ecut2.in

#selecting the type of Bravais lattice
if [ $brav = "FCC" ]
then
 sed -i '/shiftk/ r FCCshift' ecut2.in
 sed -i 's/nshiftk/nshiftk  4/g' ecut2.in
fi

if [ $brav = "BCC" ]
then
 sed -i '/shiftk/ r BCCshift' ecut2.in
```

```
 sed −i ’s/nshiftk/nshiftk  3/g’ ecut2.in
fi


if [ $brav = ”HL” ]
then
 sed −i ’/shiftk/ r HLshift’ ecut2.in
 sed −i ’s/nshiftk/nshiftk  2/g’ ecut2.in
fi



#calculating the initial etotal
#adding an initial ecut to the input file
sed −e ’s/ecut/ecut   ’$iecut’   /’ ecut2.in > mecut2.in

#run abinit
mpirun −np $cores abinit < ecut2.files

#edition of the output file for extracting total energy
sed −e ’s/(etotal)/et/’ −e ’s/E+/*10^/’ ecut2.out > mecut2.out
grep etotal* mecut2.out > ecut_dat

#saving total energy
ECUTARRAY1=(‘cat ”ecut_dat”‘)
iecut=$(echo ”scale=6; $iecut+$int” | bc )



#Here starts the tolerance criterion evaluation
while [ $ecutfound −eq 0 ]

 do
 rm −f mecut2.in mecut2.out ecut_dat

 #changing the value of ecut
 sed −e ’s/ecut /ecut ’$iecut’   /’ ecut2.in > mecut2.in

 #run abinit
 mpirun −np $cores abinit < ecut2.files

 #edition of the output file
 sed −e ’s/(etotal)/et/’ −e ’s/E+/*10^/’ ecut2.out > mecut2.out
 grep etotal* mecut2.out > ecut_dat

 #saving the total energy
```

```bash
ECUTARRAY2=(`cat "ecut_dat"`)
resta=$( echo "scale=6; ${ECUTARRAY2[1]#-} - ${ECUTARRAY1[1]#-}" | bc )
resta=${resta#-}

        #evaluating the tolerance criterion
        if [ 1 -eq $( echo " $resta < $tol " | bc ) ]
         then etotalfinal=${ECUTARRAY1[1]}
               ecutfound=1    #tolerance achieved
               ecutfinal=$iecut
        fi

 iecut=$( echo "scale=6; $iecut+$int" | bc )
 ECUTARRAY1[1]=${ECUTARRAY2[1]}
done

echo Finished!! the converged ecut is $ecutfinal with total energy $etotalfinal


cd ../

#erasing previous file with the information of other converged ecut
if [ -f "ecutenergy" ]
 then
    rm "ecutenergy"
 fi

#saving the converged ecut in a text file
echo $ecutfinal>>energycut
```

B SCRIPT FOR EXTRACTING AND ORDERING THE QUASIPARTICLE ENERGIES

B.1 Bash script for extracting the quasiparticle energies of the output files

```
#adding general parameters to abinit input file
sed -i '/#general parameters/ r general_param.cdl' finalgw.in
sed -e 's/ngkpt/ngkpt  '$grid' '$grid' '$grid' /g' -i finalgw.in
sed -i 's/nkptgw/nkptgw  '$n_kpt' /g' finalgw.in

#adding k-points and the specific bands
sed -i '/\<kptgw\>/ r kp_SCR' finalgw.in
sed -i '/bdgw/ r bandsGW' finalgw.in

#message that appears in screen to inform that the calculation have started
echo
echo -e "\e[1;36mCALCULATING_GW_CORRECTION\e[0m_"
echo

#abinit calculation
mpirun -np $cores abinit < GW_x.files > log_GW

cp finalgw.out finalgw-$grid-$n_kpt-$sys-.out
rm -f GWinformation-$n_kpt-$sys

#extracting the relevant information of the output file and saving in a text file v
grep -A $n_bands "Band_____E0" finalgw-$grid-$n_kpt-$sys-.out > GWinformation

#erasing undesired characters
sed -i '/Band/d' ./GWinformation
sed -i '/--/d' ./GWinformation
```

49

cp GWinformation GWinformation−$n_kpt−$sys 2> /dev/null

B.2 Python script to order the quasiparticle energies

```python
import numpy as np
import sys

#number of k−points and bands
n_kpt=int(sys.argv[1])
n_bands=int(sys.argv[2])

GWinfo=np.loadtxt('GWinformation')  #from the abinit output file
DFTinfo=np.loadtxt('bndDFT')    #LDA eigen−energies
DFTwGW=np.loadtxt('DFTbndener')

#matrix that will contain the quasiparticle energies
GW=np.zeros((n_kpt,n_bands+1))
diff=np.linspace(0,0,n_bands)
GWbnds=np.linspace(1,n_kpt,n_kpt)

GW[:,0]=GWbnds

#adding quasiparticle energies
j=0
for i in range(0,n_kpt):
 GW[i,1:n_bands+1]=GWinfo[j:j+n_bands,9]
 j=j+n_bands
 #print i

#ordering energies
for l in range(0,n_kpt):
 GW[l,1:n_bands]=sorted(GW[l,1:n_bands])

#save quasiparticle energies in a texfile
np.savetxt('bndGW',GW,"%.3f")

#calculating the energy corrections
for i in range (0,n_bands):
 a=DFTinfo[:,i+1]
 b=GW[:,i+1]
 res=b−a;
 diff[i]=np.mean(res)
 DFTwGW[:,i+1]=DFTwGW[:,i+1]+diff[i]
```

```
#saving the energy corrections
np.savetxt('DFTwGW',DFTwGW,"%.3f")    #to plot the k−point over the path
np.savetxt('diff',diff,"%.3f")
```

Bibliography

[1] P Sarantos. The computerized models in physics teaching: Computational physics and ict. 04 2019.

[2] C Klingenberg. Grand challenges in computational physics. *Frontiers in Physics*, 1:2, 2013.

[3] S. Plimpton. Computational limits of classical molecular dynamics simulations. *Computational Materials Science*, 4(4):361 – 364, 1995. Proceedings of the Workshop on Glasses and The Glass Transition:1 Challenges in Materials Theory and Simulation.

[4] A. Goñi R. Gelpí, J. Hospital and M. Orozco. Molecular dynamics simulations: Advances and applications. *Advances and Applications in Bioinformatics and Chemistry*, 10:37, 11 2015.

[5] G. Boulanger P. Cannuccia E. Marini A. Côté M. Poncé, S. Antonius and X. Gonze. Verification of first-principles codes: Comparison of total energies, phonon frequencies, electron–phonon coupling and zero-point motion correction to the gap between abinit and qe/yambo. *Computational Materials Science*, 83:341 – 348, 2014.

[6] N. Harrison. An introduction to density functional theory. 2019.

[7] F. Fiolhais, C. Nogueira and M. Marques. *A Primer in Density Functional Theory*. Springer, 1 edition, 2003.

[8] R. Martin. *Electronic Structure*. Cambridge University Press, 1 edition, 2014.

[9] A. Ruzsinszky and P. Perdew. Twelve outstanding problems in ground-state density functional theory: A bouquet of puzzles. *Computational and Theoretical Chemistry*, 963(1):2 – 6, 2011.

[10] I. Yakovkin and P. Dowben. *Surface Review and Letters (SRL)*, pages 481–487.

[11] P. Perdew. Density functional theory and the band gap problem. *International Journal of Quantum Chemistry*, 30:451 – 451, 1986.

[12] A. Kurt and N. Ashcroft. Corrections to density-functional theory band gaps. *Phys. Rev. B*, 58(23), 1998.

[13] W. Precker and A. da Silva. Experimental estimation of the band gap in silicon and germanium from the temperature-voltage curve of diode thermometers. *American Journal of Physics - AMER J PHYS*, 70:1150–1153, 11 2002.

[14] Z. Moontragoon, P. Ikonic and P. Harrison. Band structure calculations of si-ge-sn alloys: Achieving direct band gap materials. *Semiconductor Science and Technology*, 22, 07 2007.

[15] A. Dargys and J. Kundrotas. *Handbook on Physical Properties of Ge, Si, GaAs and InP.* Science and Encyclopedia Publishers, Vilnius., 1 edition, 1994.

[16] R. Mattuck. *A Guide to Feynman Diagrams in the Many-body Problem.* Dover Books on Physics Series. Dover Publications, Incorporated, 1976.

[17] A. Fetter and J. Walecka. *Quantum Theory of Many-Particle Systems.* McGraw-Hill, New York, 1971.

[18] L. Onida, G. Reining and A. Rubio. Electronic excitations: density-functional versus many-body green's-function approaches. *Rev. Mod. Phys.*, 74:601–659, Jun 2002.

[19] L. Abrikosov, A. Gorkov and E. Dzyaloshinskii. *Methods of quantum field theory in statistical physics.* Dover, New-York, 1975.

[20] W. Kutzelnigg. *The Many-Body Perturbation Theory of Brueckner and Goldstone.* Springer US, Boston, MA, 1992.

[21] L. Hedin. New method for calculating the one-particle green's function with application to the electron-gas problem. *Phys. Rev.*, 139(3A):A796–A823, August 1965.

[22] L. Reining. The gw approximation: content, successes and limitations: The gw approximation. *Wiley Interdisciplinary Reviews: Computational Molecular Science*, 8:e1344, 12 2017.

[23] N. Wiser. Dielectric constant with local field effects included. *Phys. Rev.*, 129(1):62–69, January 1963.

[24] L. Adler. Quantum theory of the dielectric constant in real solids. *Phys. Rev.*, 126(2):413–420, April 1962.

[25] R. Hott. Gw -approximation energies and hartree-fock bands of semiconductors. *Physical review. B, Condensed matter*, 44:1057–1065, 08 1991.

[26] C. Grüning M. Marini, A. Hogan and D. Varsano. Yambo: An ab initio tool for excited state calculations. *Computer Physics Communications*, 180:1392–1403, 08 2009.

[27] N. Bruneval, F. Vast and L. Reining. Effect of self-consistency on quasiparticles in solids. *Phys. Rev. B*, 74:045102, Jul 2006.

[28] F. et al. Gonze, X. Jollet. Recent developments in the ABINIT software package. *Comput. Phys. Commun.*, 205:106–131, August 2016.

[29] G. et al. Gonze, X. Rignanese. A brief introduction to the ABINIT software package. *Zeitschrift für Kristallographie - Crystalline Materials*, 220([U+215A]):558–562, January 2005.

[30] X. et al Gonze, X. Amadon. ABINIT: First-principles approach to material and nanosystem properties. *Comput. Phys. Commun.*, 180(12):2582–2615, December 2009.

[31] O. et al. Giannozzi, P. Andreussi. Advanced capabilities for materials modelling with quantum espresso. *Journal of Physics: Condensed Matter*, 29(46):465901, 2017.

[32] B. et al. Paolo, G. Stefano. Quantum espresso: a modular and open-source software project for quantum simulations of materials. *Journal of Physics: Condensed Matter*, 21(39):395502 (19pp), 2009.

[33] P. Hohenberg and W. Kohn. Inhomogeneous electron gas. *Phys. Rev.*, 136:B864–B871, Nov 1964.

[34] W. Kohn and L. J. Sham. Self-consistent equations including exchange and correlation effects. *Phys. Rev.*, 140:A1133–A1138, Nov 1965.

[35] P. Dirac. Note on exchange phenomena in the thomas atom. *Mathematical Proceedings of the Cambridge Philosophical Society*, 26:376–385, 1930.

[36] R. Feynman. Space-time approach to quantum electrodynamics. *Phys. Rev.*, 76:769–789, Sep 1949.

[37] J. Schwinger. On quantum-electrodynamics and the magnetic moment of the electron. *Phys. Rev.*, 73:416–417, Feb 1948.

[38] S. Tomonaga. Development of quantum electrodynamics. *Science*, 154(3751):864–868, 1966.

[39] L. Hedin and S. Lundqvist. *Effects of Electron-Electron and Electron-Phonon Interactions on the One-Electron States of Solids*, volume 23, pages 1–181. Academic Press, 1969.

[40] F. Dyson. The s matrix in quantum electrodynamics. *Phys. Rev.*, 75:1736–1755, Jun 1949.

[41] J. Schwinger. On the Green's Functions of Quantized Fields. I. *Proceedings of the National Academy of Science*, 37:452–455, July 1951.

[42] L. Onida G. Pulci, O. Reining and R. Del Sole. Many-body effects on one-electron energies and wave functions in low-dimensional systems. *Computational Materials Science*, 20(3):300 – 304, 2001. 9th Int. Workshop on Computational Materials Science.

[43] N. Wiser. Dielectric constant with local field effects included. *Phys. Rev.*, 129:62–69, Jan 1963.

[44] M. Luppi E. Hogan C. Garbuio V. Sottile F. Magri R. Pulci, O. Marsili and R. Del Sole. Electronic excitations in solids: Density functional and green's function theory. *physica status solidi (b)*, 242:2737 – 2750, 11 2005.

[45] J. Mendoza B. Cabellos and T. Gordillo. Tiniba: Programas para el cálculo en paralelo de respuestas Ópticas en semiconductors usando un cluster de computo. Registrado ante el Instituto Nacional de Derechos de Autor (INDAUTOR-México) con número de registro 03-2009-120114033400-01.

[46] J. Monkhorst and D. Pack. Special points for brillouin-zone integrations. *Phys. Rev. B*, 13:5188–5192, Jun 1976.

[47] B. Alouani M. Lebègue, S. Arnaud and P. Bloechl. Implementation of an all-electron gw approximation based on the projector augmented wave method without plasmon pole approximation: Application to si, sic, alas, inas, nah, and kh. *Phys. Rev. B*, 67:155208, Apr 2003.

[48] T. van Schilfgaarde, M. Kotani and S. Faleev. Quasiparticle self-consistent *gw* theory. *Phys. Rev. Lett.*, 96:226402, Jun 2006.

[49] M. Crowley, J. Tahir-Kheli, and W. Goddard. Resolution of the band gap prediction problem for materials design. *The Journal of Physical Chemistry Letters*, 7(7):1198–1203, 2016. PMID: 26944092.

[50] A. Pippard. An experimental determination of the fermi surface in copper. *Philosophical Transactions of the Royal Society of London. Series A, Mathematical and Physical Sciences*, 250(979):325–357, 1957.

[51] P. Guczi, L. Zoltán and P. Gábor. Chapter 4 - metal nanoclusters: Electronic aspects and physico-chemical characterization. In B. CORAIN, G. SCHMID, and N. TOSHIMA, editors, *Metal Nanoclusters in Catalysis and Materials Science*, pages 77 – 105. Elsevier, Amsterdam, 2008.

[52] D. Aspnes and A. Studna. Dielectric functions and optical parameters of si, ge, gap, gaas, gasb, inp, inas, and insb from 1.5 to 6.0 ev. *Phys. Rev. B*, 27:985–1009, Jan 1983.

[53] C. Olguín, P. Angammana and S. Jayaram. Experimental study of dielectric properties of fumed silica/silicone composites. pages 683–686, 10 2016.

[54] B. Johnson T. Shelton D. Sang-Hyun. Boreman G. Olmon, R. Slovick and M. Raschke. Optical dielectric function of gold. *Phys. Rev. B*, 86:235147, Dec 2012.

[55] J. Sundheimer M. Tucker E. Boreman-G. Yang, H. D'Archangel and M. Raschke. Optical dielectric function of silver. *Phys. Rev. B*, 91:235137, Jun 2015.